Theory of Ferromagnetism driven by superexchange in Dilute Magnetic Semiconductors

JEMS 2013 Joint European Magnetic Symposia

Mon 26 Aug 2013
(17:15 - 17:30)

25-30 August 2013
Rodos Palace Convention Center
Rhodes, Greece

C. Simserides [1], J.A. Majewski [2], K.N. Trohidou [3], T. Dietl [2,4,5]

1. Physics Department, University of Athens, Greece

2. Institute of Theoretical Physics, University of Warsaw, Poland

3. Institute for Advanced Materials, Physicochemical Processes, Nanotechnology & Microsystems, NCSR Demokritos, Athens, Greece

4. Institute of Physics, Polish Academy of Sciences, Warszawa, Poland

5. WPI-Advanced Institute for Materials Research, Tohoku University, Sendai, Japan

Acknowledgements
FunDMS Advanced Grant of the ERC (Grant No. 227690), Ideas 7th Framework Programme of European Community.
Computer time in Athens partly provided by the National Grid Infrastructure HellasGrid.

summary

theoretically study ferromagnetism in $Ga_{1-x}Mn_xN$

Tight Binding:

determine exchange integrals J_{ij} : Mn Spins i & j @ distances R_{ij}
up to 16th NN in zb GaN

experimentally determined input parameters

- no itinerant carriers
- ferromagnetic superexchange between Mn^{3+} (for all explored R_{ij})

Monte Carlo:

extensive simulations determine T_C (cumulant crossing method)

Our predictions for $T_C(x)$ quantitative agreement with experimental data
(randomly distributed Mn^{3+} , $0.01 < x < 0.1$)

Conclusion: ferromagnetic superexchange

Mn acceptor binding energy in III-V compounds

GaN: deep hole trap formed

⇒ no itinerant holes

⇒ no efficient ferro-magnetism

according to *p-d* Zener model

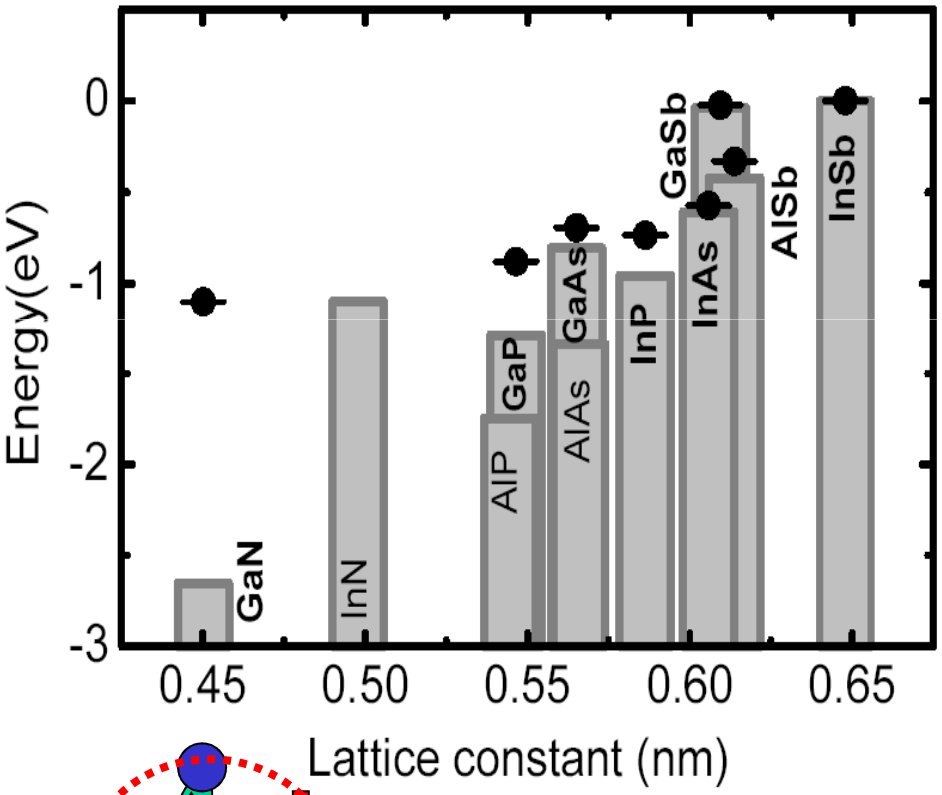

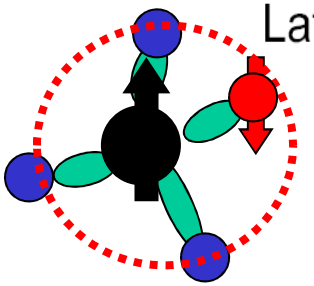

Dietl *et al.*
PRB 66 (2002) 033203

Mn^{3+} energy diagram . . .

Mn substituting a trivalent metal

d^4 (Mn^{3+} e.g. in GaN) *or* $d^5 + h$ (e.g. Mn^{2+} in GaAs)

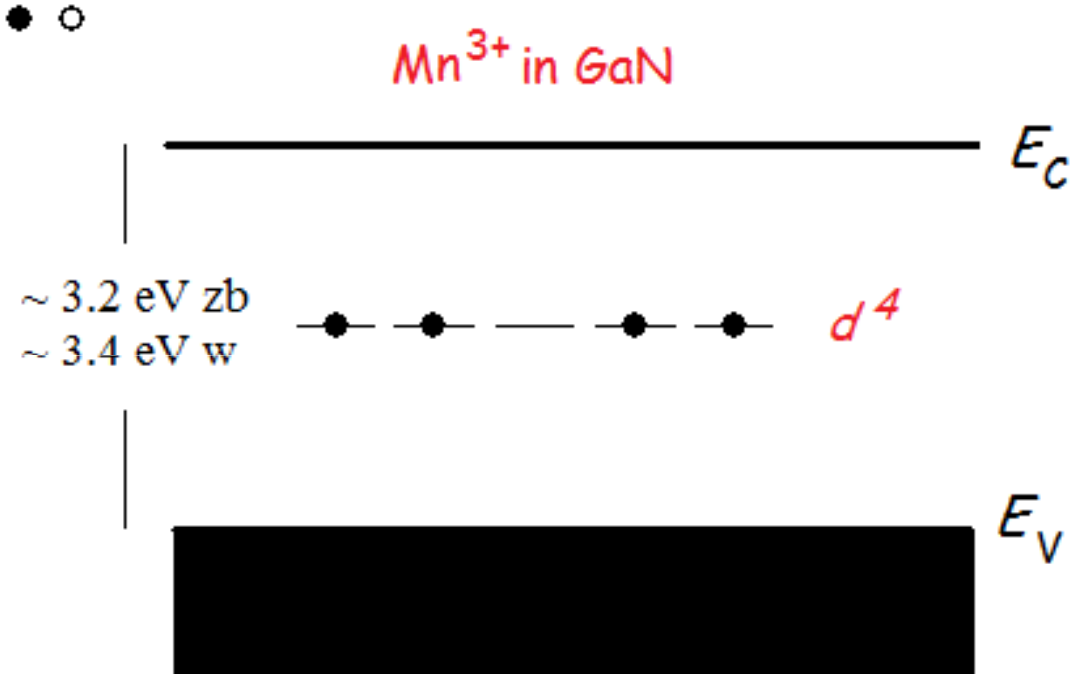

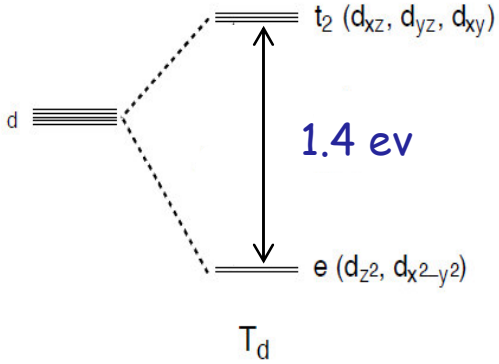

for weak compensation
by donors remains Mn^{3+}

(Ga,Mn)N – dilute ferromagnetic insulator

Mn^{2+} in II-VI antiferromagnetic superexchange

Mn substitutes cations (Cd, Zn, . . .)

local magnetic moments ONLY! no holes

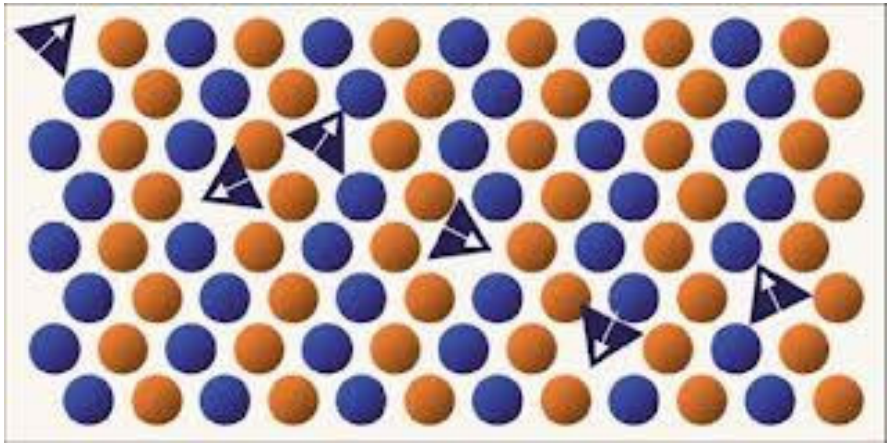

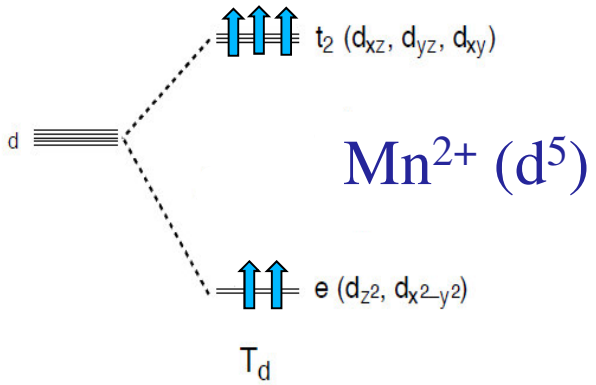

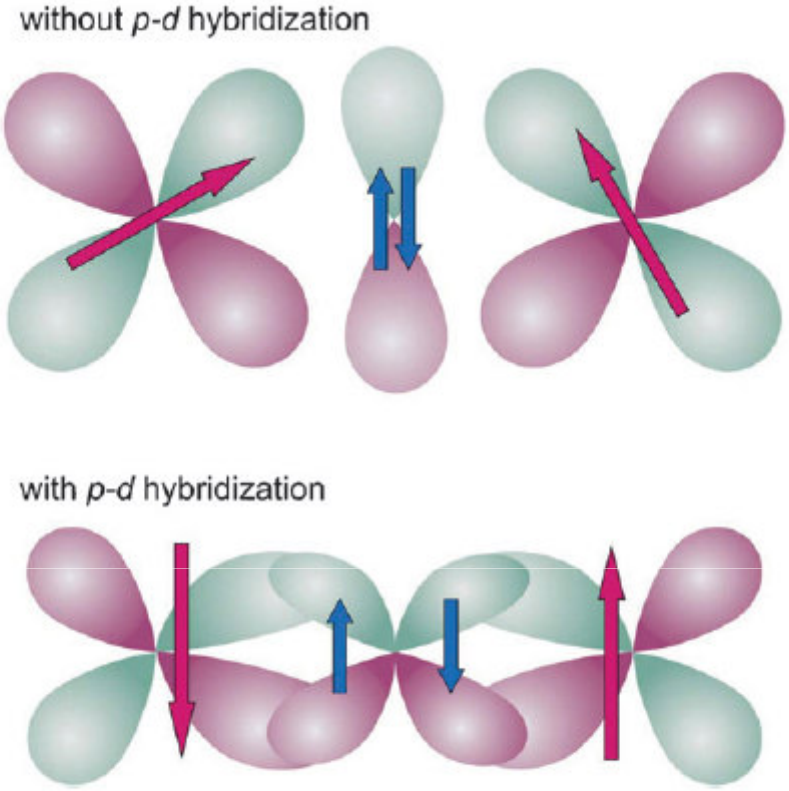

Fig. 5 Schematic illustration of the antiferromagnetic superexchange between spins (red arrows) localised on open *d* shells, mediated *via* the *p*–*d* hybridisation by entirely occupied anion *p* states. A spin-dependent shift of the orbitals, occurring for an antiferromagnetic arrangement of neighbour Mn spins (lower panel), enhances the lowering of the system energy associated with the *p*–*d* hybridisation.

532 | *Chem. Soc. Rev.*, 2010, **39**, 528–539

Bonanni and Dietl

Mn^{3+} in GaN Cr^{2+} in II-VI DMS ferromagnetic coupling

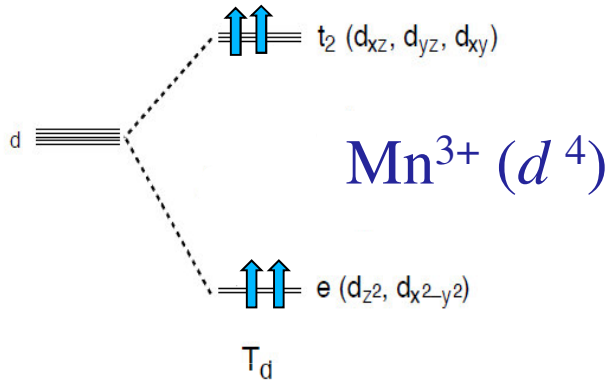

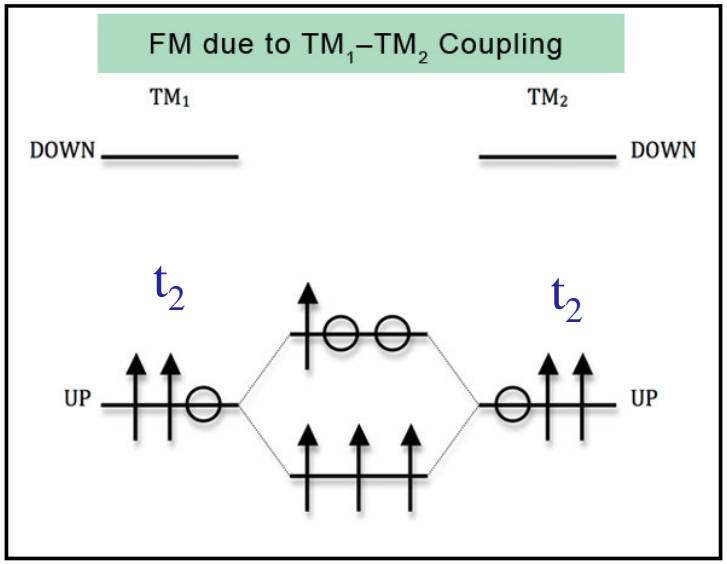

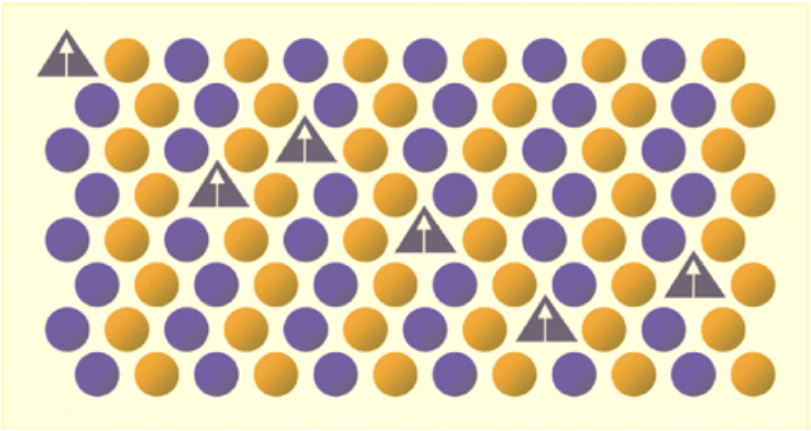

Energy level diagram describing the stabilization of the ferromagnetic spin arrangement as a result of the interaction between two hybrid orbitals located on two impurities, here labeled TM1 and TM2, in a **tetrahedral semiconductor**.
In the case of partial occupancy of the individual hybrid orbitals, the ferromagnetic configuration is stabilized by the preferential filling of the lower energy state.

Zunger Lany Raebiger Physics 3, 53 (2010)

ab initio nn Mn-Mn exchange energy

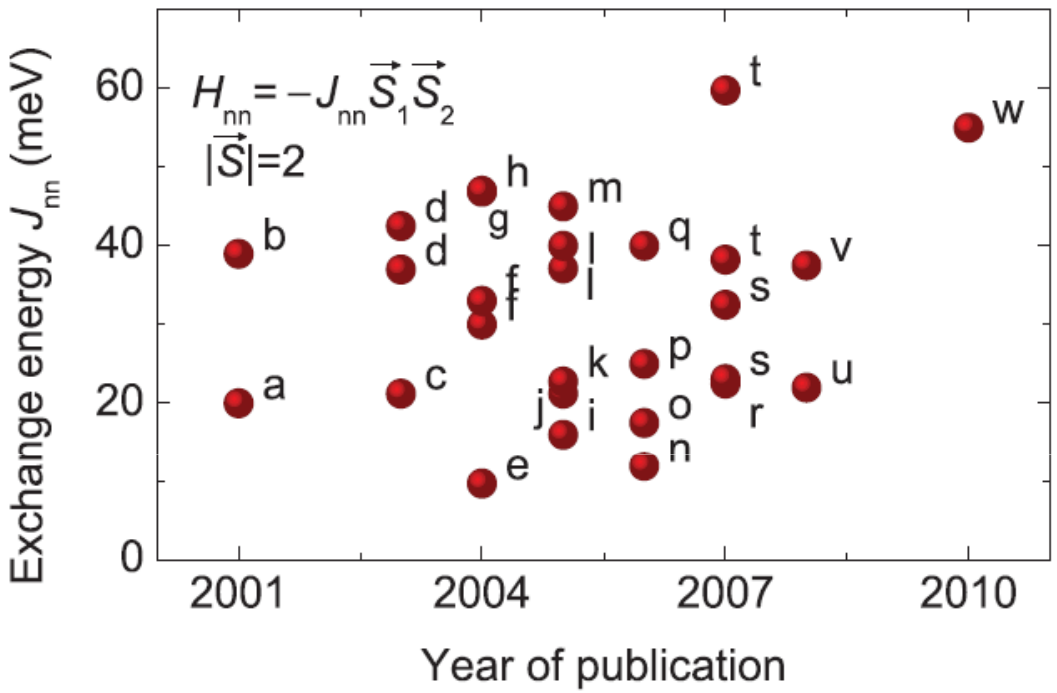

assigned to double exchange

a Sato and Katayama-Yoshida (2001)
b v. Schilfgaarde and Mryasov (2001)
c Uspenskii et al. (2003)
d Sanyal et al., (2003);
e Q.Wang, et al. (2004);
f M. Wierzbowska, et al. (2004);
g Mahadevan and Zunger, (2004);
h Zhao, et al. (2004);
i Bergqvist et al.(2005);
j Boguslawski and Bernholc (2005);
k Sato, et al.(2005);
l Kang, et al., (2005);
m Luo and Martin, (2005);
n Marques et al. (2006);
o Tan-don et al. (2006);
p Hynninen et al. (2006);
q Kang et al. (2006);
r Larson and Satpathy (2007);
s Cui et al. (2007);
t Hynninen et al. (2007);
u Larson et al. (2008);
v Chan et al. (2008).
w Gonzalez Szawacki et al. (2011)

$Ga_{1-x}Mn_xN$ exp Curie temperature

T_C up to 13 K at x = 10%

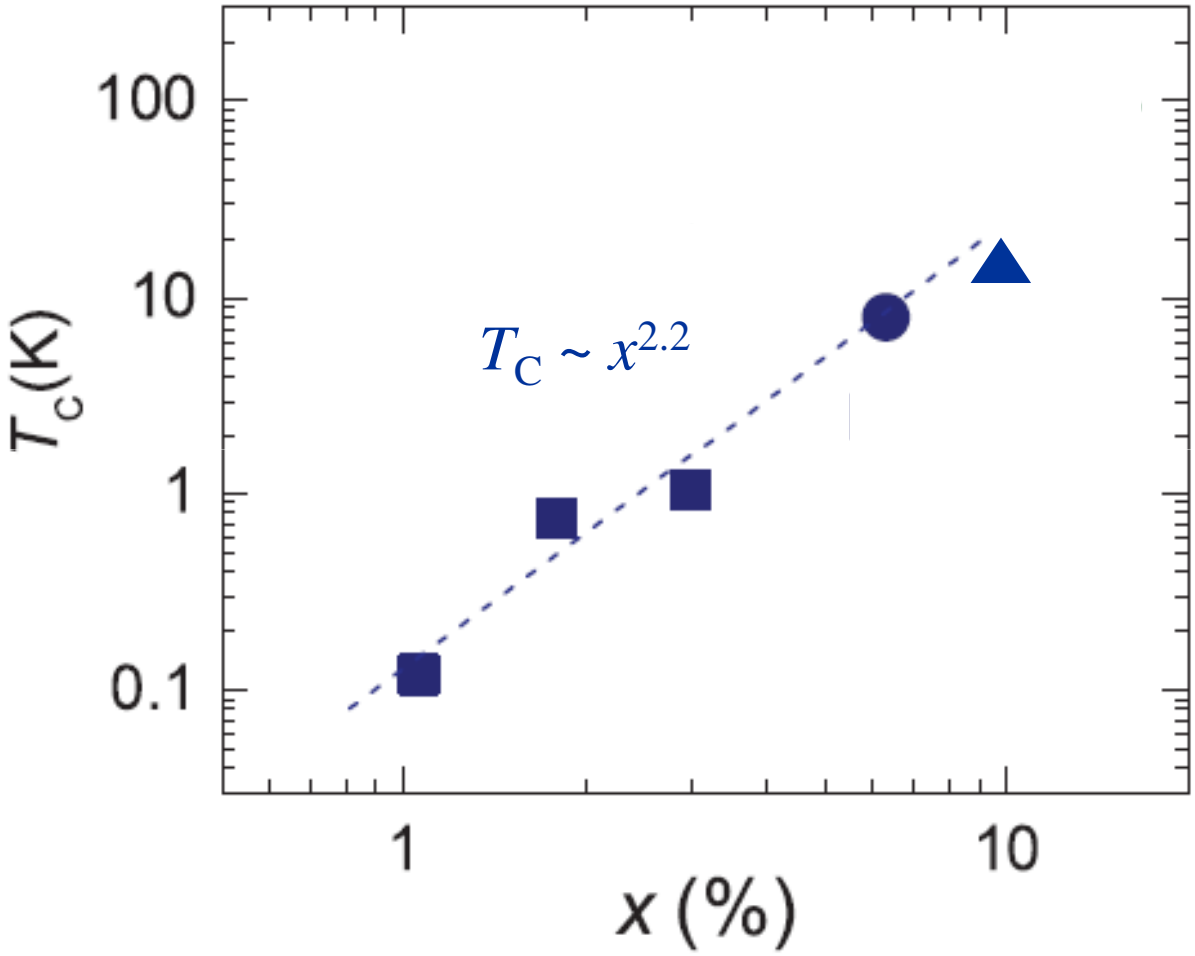

- M. Sawicki et al. [Warsaw, Linz] PRB'12
- E. Sarigiannidou et al. [Grenoble PRB'06]
- G. Kunert et al [Bremen, Warsaw, Linz] APL'12

$Ga_{1-x}Mn_xN$ exp vs. *ab initio* theory Curie temperature

T_C up to 13 K at x = 10%

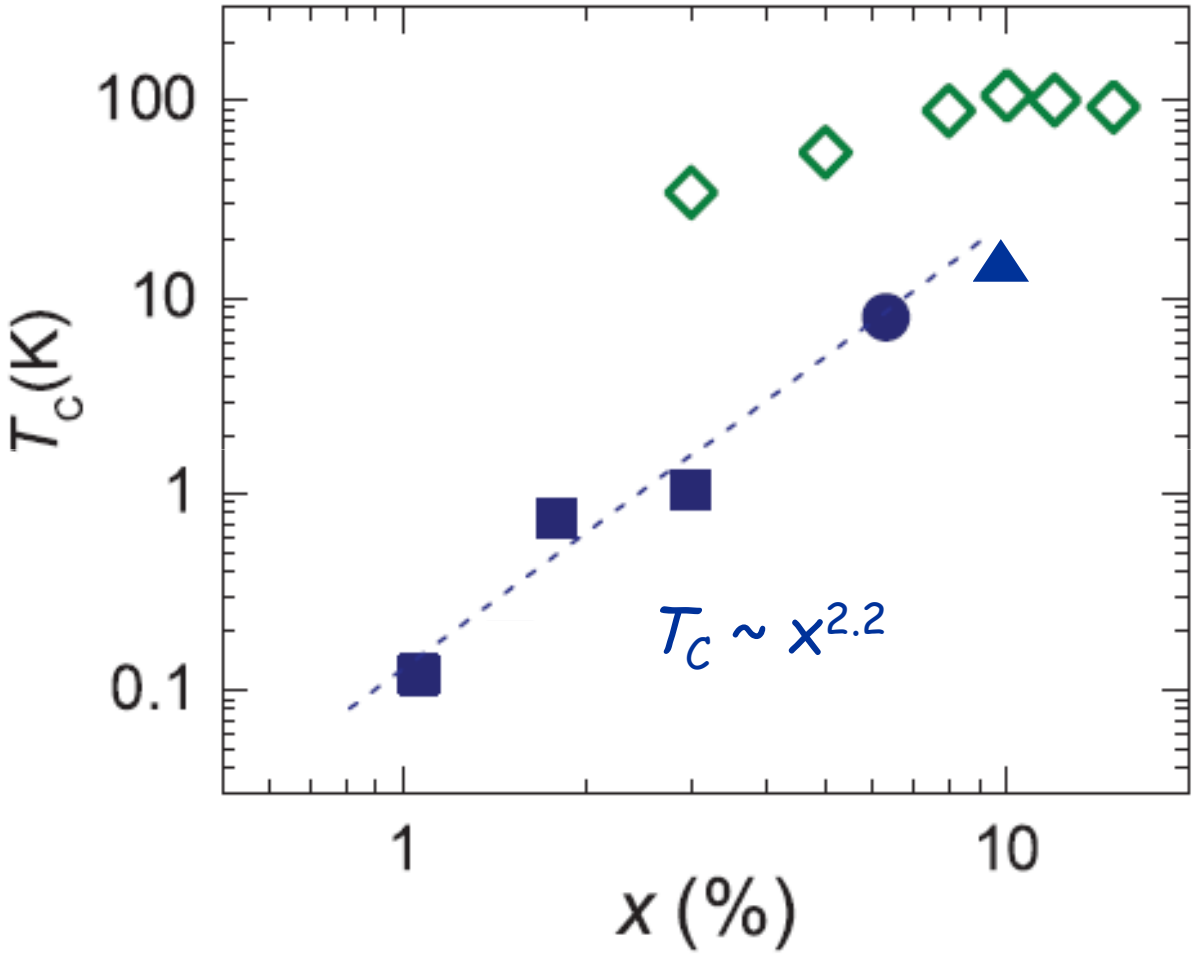

ab initio: K. Sato et al. [Osaka] RMP 2010

■ M. Sawicki et al. [Warsaw, Linz] PRB 2012

● E. Sarigiannidou et al. [Grenoble PRB 2006]

▲ G. Kunert et al [Bremen, Warsaw, Linz] APL'12

DFT computations:
1. T_C is much too high (LSDA overestimates *p-d* hybridization)
2. Trend NOT OK

Hence . . .

tight binding approximation

. . . . . ⇒

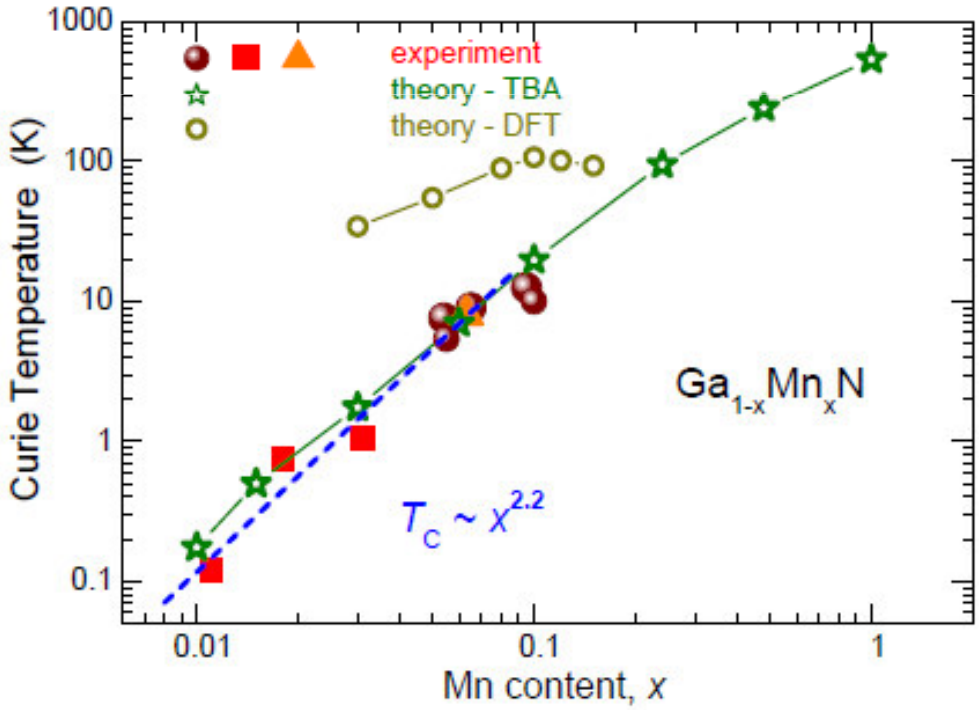

S. Stefanowicz et al [Warsaw, Bremen, Linz, Athens] PRB'13 (RC)

$Ga_xMn_{1-x}N$ ferromagnetic superexchange

Cr-doped zb zinc chalcogenides (ZnS, ZnSe, ZnTe)
Blinowski, Kacman, Majewski Phys. Rev. B 53, 9524 (1996)

This theory can be adopted for Mn-doped zincblende GaN.

Element or Ion	Electron Configuration	Spin	
Cr	[Ar] $3d^5\ 4s^1$		
Mn	[Ar] $3d^5\ 4s^2$		
Cr^{2+}	[Ar] $3d^4$	2	substitutional Cr-doped zb zinc chalcogenides
Mn^{3+}	[Ar] $3d^4$	2	substitutional Mn-doped zb GaN

no hole is created by a substitutional Mn_{Ga}

Experiments

[Sawicki *et al.*, Phys. Rev. B 85, 205204 (2012), Stefanowicz *et al.*, Phys. Rev. B 88, 081201(R) (2013)] :

(i) ~ all Mn^{3+}, substitutionally incorporated — lack of mixed valence => **NO double exchange**

(ii) highly resistive material even at 300 K — no electrons and holes around => **NO Zener exchange**

⇒ **superexchange**

sign determined by Anderson-Goodenough-Kanamori rules

Method of J_{ij} calculation

4th-order perturbation in V_{pd} $\forall$ orbital configurations γ and δ

interaction between Mn_{Ga} spins $-k_B \sum_{\alpha,\beta} J_{\alpha\beta}^{\gamma\delta}(\boldsymbol{R}_{12})\, S_{1\alpha}\, S_{2\beta}$

γ (δ) : which t_2 orbital (d_{yz}, d_{xz}, d_{xy}) remains empty @ 1 (2) ion α (β): x, y, z

Mn^{3+} ground state: 1 of 3 possible orbital singlets tetragonal Jahn-Teller distortions (x, y, z)
4 out of 5 d orbitals singly occupied 2 e & 2 of 3 t_2

unperturbed magnetic ions: Parmenter Hamiltonian

unperturbed band states: empirical TBA $sp^3 s^*$

superexchange tensor

$$J_{\alpha\beta}^{\gamma\delta}(\mathbf{R}_{12}) = F_{\alpha\beta}^{\gamma\delta}(\mathbf{R}_{12}) + H_{\alpha\beta}^{\gamma\delta}(\mathbf{R}_{12}) + G_{\alpha\beta}^{\gamma\delta}(\mathbf{R}_{12})$$

between occupied orbitals (F)

occupied orbitals - empty orbital (H)

between empty orbitals (G)

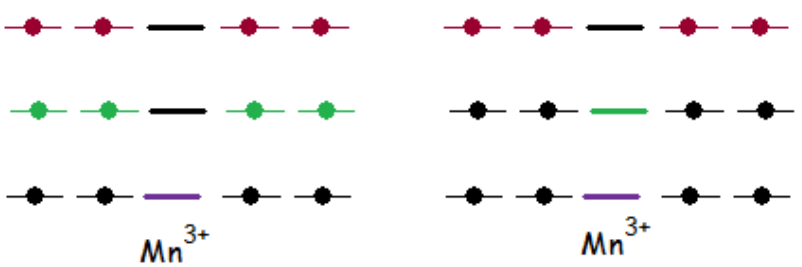

Then, we determine the average of $J_{\alpha\beta}^{\gamma\delta}$ @ given distance $R_{ij} \Rightarrow J_{ij}$

Parmenter Hamiltonian …

for a given eigenvalue of N

the eigenvalue of $H_0 + H'_{ee}$ E_N^S

is minimized by maximizing the eigenvalue of $\vec{S} \cdot \vec{S}$

(Hund's rule satisfied)

That portion of the total Hamiltonian describing the localized center by itself can be taken as

$$H_0 + H'_{ee} = (\epsilon_0 + J - \tfrac{1}{2}U)N + \tfrac{1}{2}(U - \tfrac{1}{2}J)N^2 - J\vec{S} \cdot \vec{S} \,. \quad (30)$$

rotationally invariant Parmenter Hamiltonian

different energies $E_N{}^S$ to states with different total spin values S of the N d electrons

Parmenter, Phys. Rev. B **8, 1273 (1973)**

Method of J_{ij} calculation

Charge transfer energy between Mn ion & top of valence band $e_1 = -1.8$ eV
On-site correlation energy for Mn^{3+} ions $U = 1$ eV
On-site exchange energy for Mn^{2+} ions, $\Delta = E(S = 5/2) - E(S = 3/2) = 2$ eV
Charge transfer parameter $e_2 = 4.8$ eV,
uncertainty of e_1 and e_2 ~ 0.5 eV

$V_{pd\sigma} = -1.5 \pm 0.1$ eV
$V_{sp\sigma} = -1.5$ eV
$V_{pp\pi} = 0.675$ eV
$V_{pp\sigma} = -1.62$ eV

Parameters taken from experiments
Graf et al., Phys. Status Solidi B **239**, 277 (2003)
Han et al., Appl. Phys. Lett. **86**, 042505 (2005)
Hwang et al., Phys. Rev. B **72**, 085216 (2005)

1st (2nd) set of J_{ij}
$e_2 = 4.8$ eV (4.4 eV) & 10 NN (16 NN)

the change of e_2 from 4.8 to 4.4 eV
is within its expected experimental uncertainty

J_{ij} can be calculated at any R_{ij}

Important!

NO supercells used

We need 16NN for percolation of x = 0.01 !

J sets

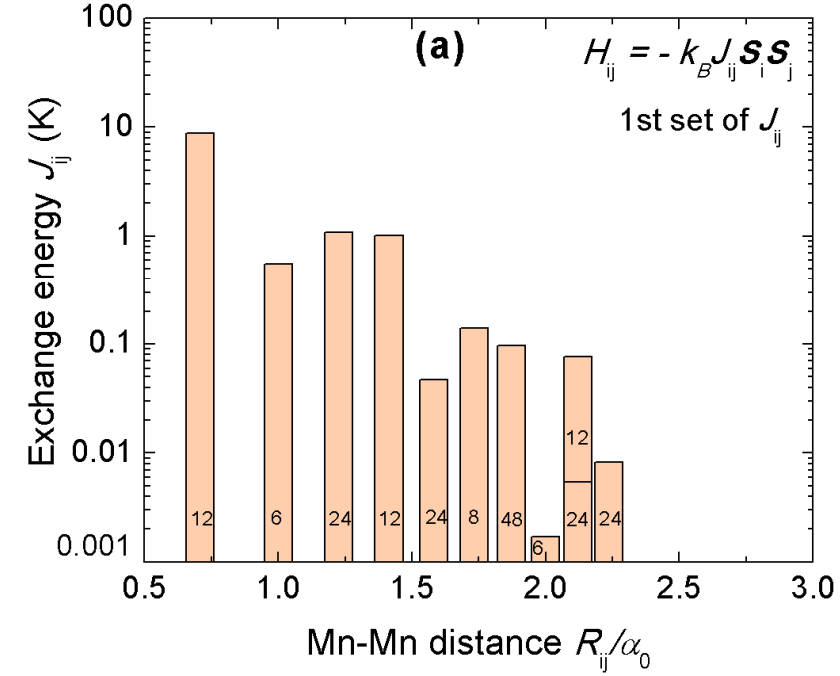

Sawicki *et al.*, Phys. Rev. B 85, 205204 (2012)

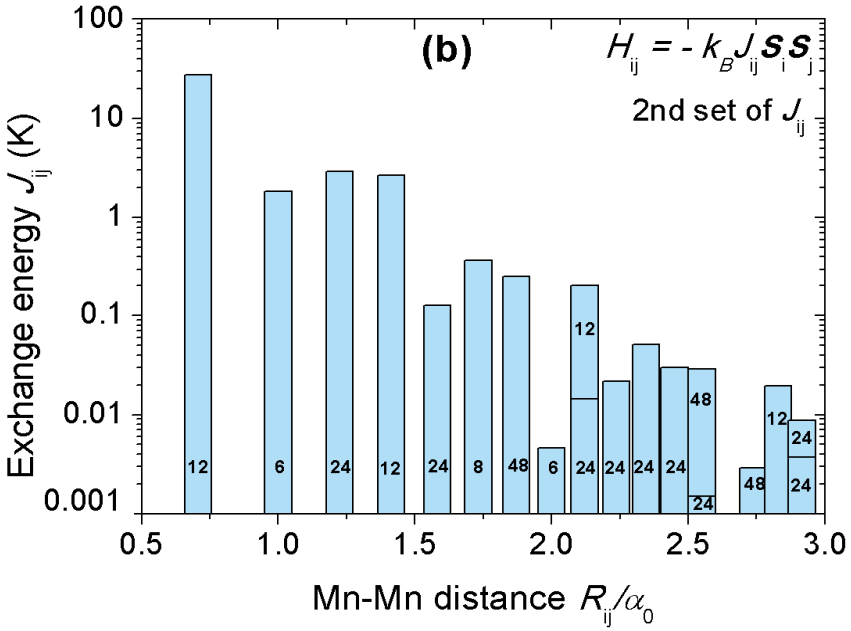

Stefanowicz *et al.*, Phys. Rev. B 88, 081201(R) (2013)

EXAMPLE $x = 0.03$ 1st set of J_{ij}

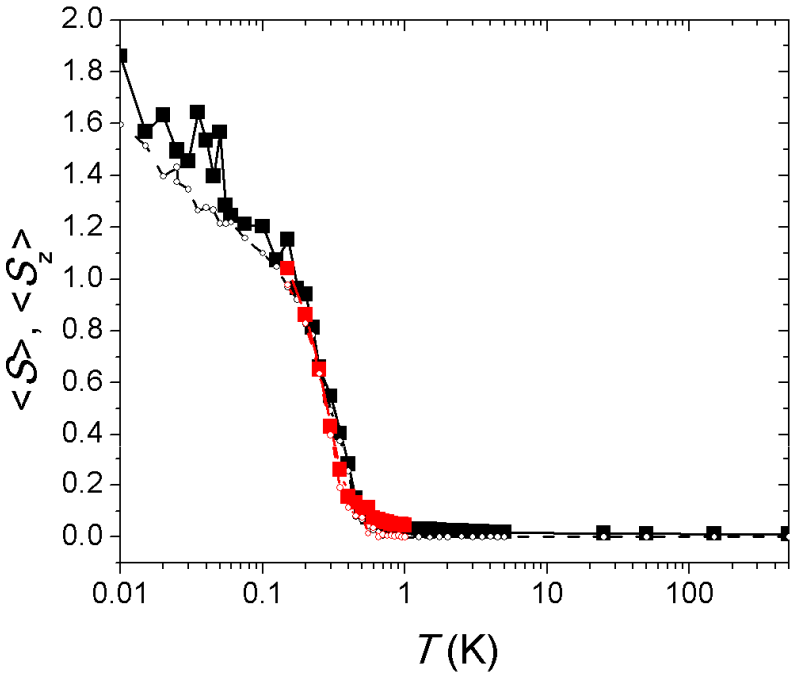

How to determine T_C?

. . .

$L = 50\ a_0$ ($N_{Mn} = 15000$)

$L = 60\ a_0$ ($N_{Mn} = 25920$)

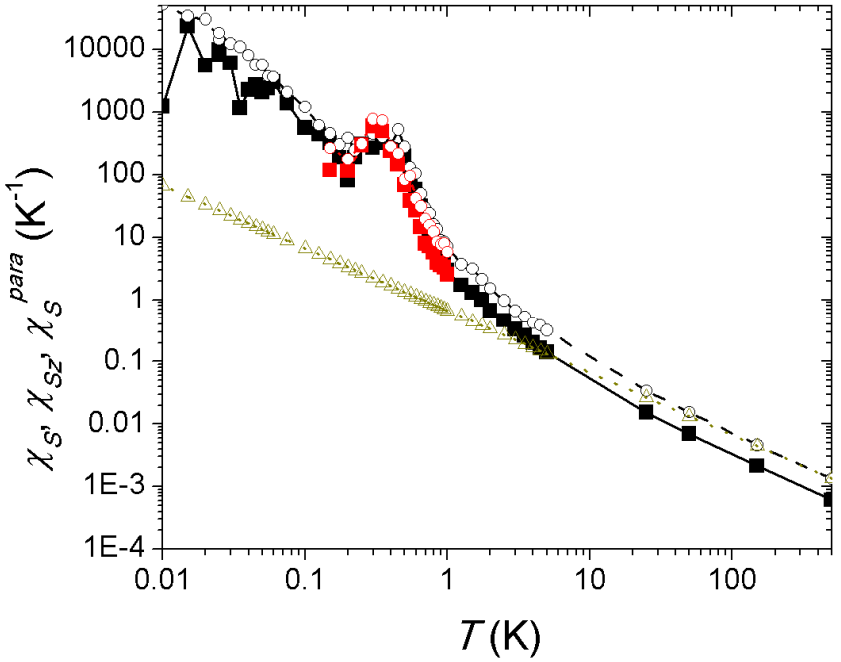

EXAMPLE $x = 0.03$ 1st set of J_{ij}
fourth order cumulant method

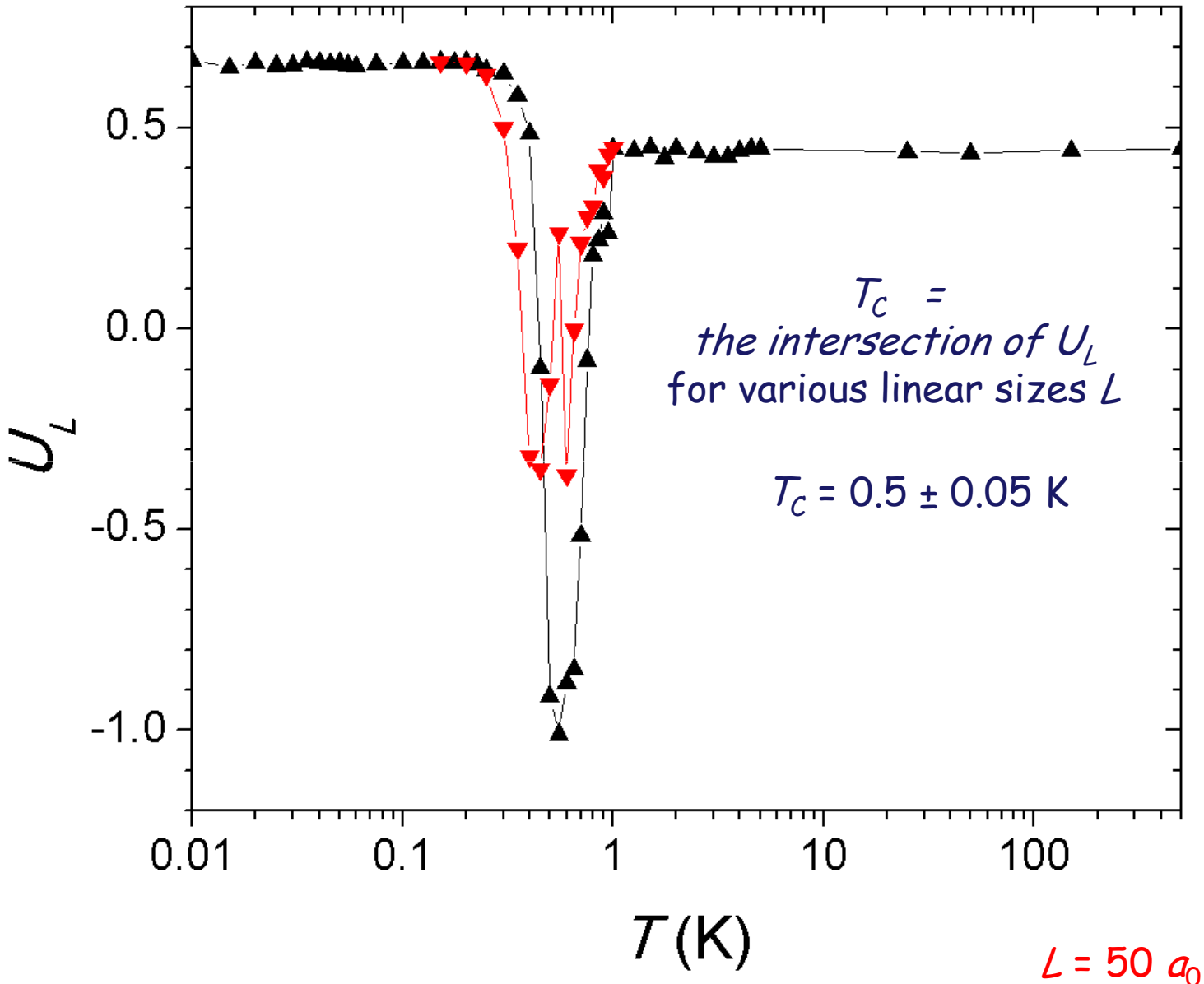

T_C = *the intersection of* U_L for various linear sizes L

$T_C = 0.5 \pm 0.05$ K

$$U_L = 1 - \frac{\langle S^4 \rangle_L}{3\langle S^2 \rangle_L^2}$$

. . .

$L = 50\ a_0$ ($N_{Mn} = 15000$)

$L = 60\ a_0$ ($N_{Mn} = 25920$)

$T_C(x)$

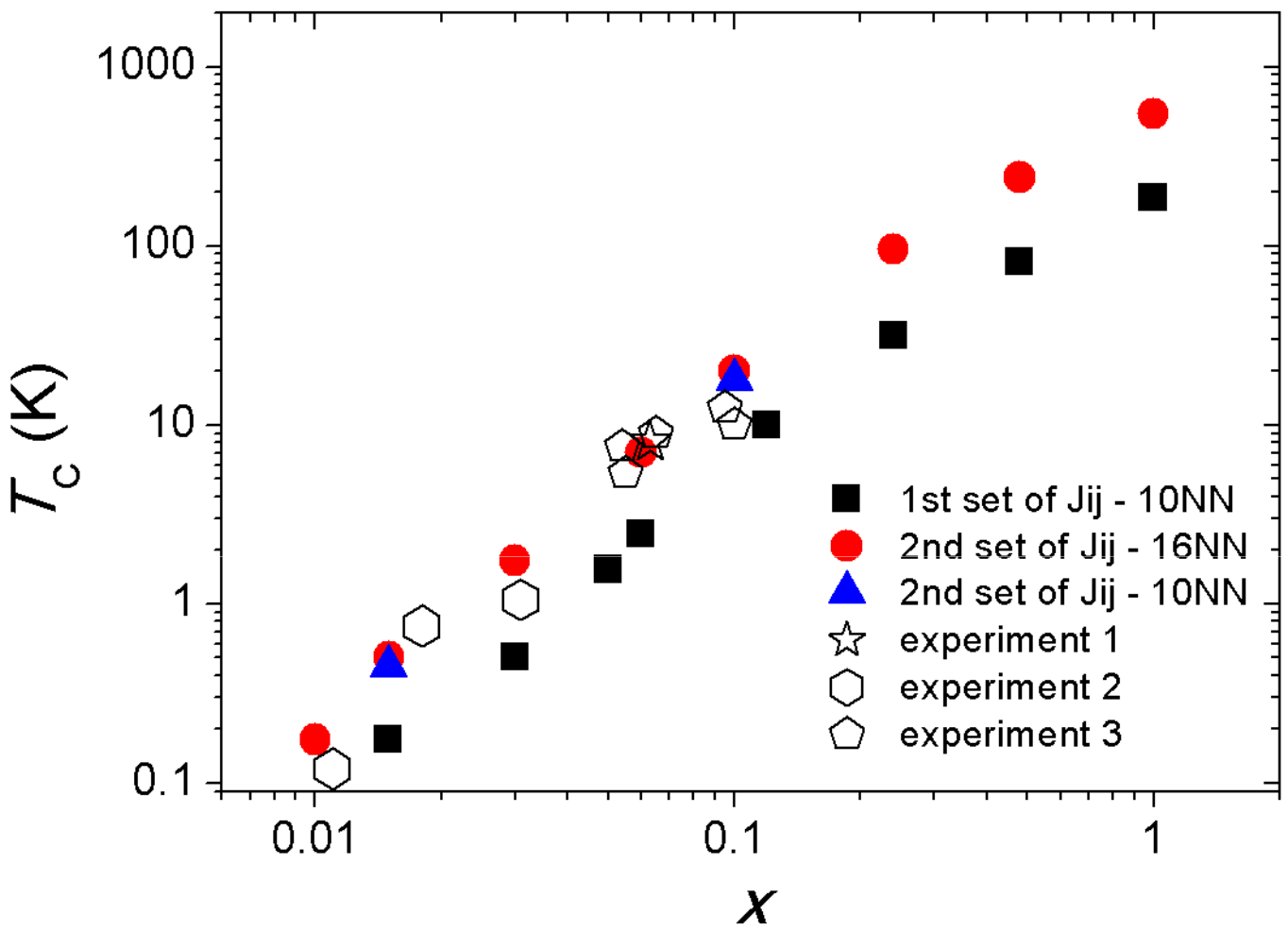

$T_C(x)$ obtained by Monte Carlo simulations using the sets of J_{ij} shown in (a-b).

$$T_C(x) \propto x^m \qquad m = 2.2 \pm 0.2$$

Conclusion

$T_C(x)$ agrees quantitatively with experiments
Mn^{3+}_{Ga} in $Ga_{1-x}Mn_xN$, $0.01 < x < 0.1$

$\Rightarrow$ ferromagnetic superexchange

$\rightarrow$ $T_C \approx 13$ K @ $x = 0.1$

$T_C(x) \propto x^m$ $m = 2.2 \pm 0.2$

both for ferromagnetic ordering (here)
partly filled t_2 states of Td coordinated TM ions

and spin-glass freezing (Mn-, Co-based II-VI DMSs)
t_2 states entirely occupied for majority spin direction

$\Rightarrow$ verifies the scaling law $m = \lambda / d$, $J_{ij} \propto R_{ij}^{-\lambda}$ d (dimensionality)

Rammal, R., and J. Souletie, 1982, Magnetism of Metals and Alloys (North-Holland)

Conclusion

Predict room-temperature ferromagnetism $x \gtrapprox 0.5$

High-T_C regime shifted to even lower x?
(ITM transition & delocalization of holes supplied by Mn ions)

Future growth effort: possible to obtain $Ga_{1-x}Mn_xN$
with randomly Mn^{3+}
& $x \gg 0.1$?

TBA vs. ab initio

our J_{ij} significantly smaller $\Rightarrow$ smaller T_C s &
stronger dependence $T_C(x)$

current *ab initio* methods **overestimate** coupling between TM levels & band states
OK here [Parmenter generalization of Anderson Hamiltonian]

within present formalism possible to compute J_{ij} for any R_{ij},

able to evaluate $T_C(x)$ down to e.g. $x = 0.01$

End

Thank you!

α-GaN vs β-GaN

α-GaN wurtzite $a = 0.3188$ nm, $c = 0.5185$ nm

Here $c/a \approx 1.626$,
ideal $c/a = (\frac{8}{3})^{1/2} \approx 1.633$.

β-GaN *zinc-blende* lattice parameter
(identical density of cation sites): $a_0 = (\sqrt{3}a^2c)^{1/3} = 0.45$ nm

	First-nearest neighbors		Second-nearest neighbors		Third-nearest neighbors	
	Number	Distance	Number	Distance	Number	Distance
fcc	12	D	6	$D\sqrt{2}$	24	$D\ (3)^{\frac{1}{2}}$
hcp	12	D	6	$D\sqrt{2}$	2	$D\ (8/3)^{\frac{1}{2}}$

D is the diameter of hard touching spheres", i.e. $D = a$ hcp

$D = \frac{\sqrt{2}}{2}a_0$ fcc

the same atomic packing factor $\pi/\sqrt{18} \approx 0.74$

almost identical *bond percolation threshold* and *site percolation threshold* for nearest neighbors

The total energy difference between α-GaN and β-GaN only ≈ 10-15 meV/atom

Hence, α-GaN can be approximated by *β*-GaN in a first decent approach.

fcc, distance of *n*th NN

$$r_n = \begin{cases} D\sqrt{n}, & n \le 13 \\ D\sqrt{n+1}, & 14 \le n \le 16 \end{cases}$$

Parmenter Hamiltonian 1

PHYSICAL REVIEW B VOLUME 8, NUMBER 3 1 AUGUST 1973

Effect of Orbital Degeneracy on the Anderson Model of a Localized Moment in a Metal

R. H. Parmenter
Department of Physics, University of Arizona, Tucson, Arizona 85721

(Received 21 March 1973)

As conventionally written, the localized-center portion of the Anderson Hamiltonian suffers from the defect of lack of rotational invariance in real space (and possibly spin space also) when describing a center with $(2l+1)$ degenerate spatial orbitals. A simple modification is suggested which restores the rotational invariance in both spaces. The eigenvalues of this localized-center portion of the Hamiltonian can be determined by inspection, and are consistent with Hund's rule. The modification leads to nontrivial changes in the properties of the full Anderson Hamiltonian. Within the context of the Hartree-Fock approximation, the likelihood of orbital broken symmetry is reduced.

a localized magnetic center

l orbital quantum number	m magnetic quantum number
$l = 2$ (d orbitals)	$m = -2, -1, 0, 1, 2$

$$N_{m0} \equiv \sum_s n_{ms} , \qquad N_{0s} \equiv \sum_m n_{ms} ,$$

$$N \equiv \sum_{ms} n_{ms} = \sum_m N_{m0} = \sum_s N_{0s} .$$

$$\vec{S} = \sum_m \vec{S}_m$$

$$\vec{L} = \sum_s \vec{L}_s$$

$$n_{ms} \equiv c_{ms}^{\dagger} c_{ms}$$

$\vec{S}_m$ being the total spin angular momentum of all electrons in orbital m, and $\vec{L}_s$ being the total orbital angular momentum of all electrons of spin s.

Parmenter Hamiltonian 2

$$H_0 = \epsilon_0 \sum_{ms} n_{ms}$$

$$H_{ee} = \tfrac{1}{2} U \sum_{s} n_{ms} n_{m,-s}$$

Anderson, one m

The electron-electron interaction Hamiltonian H_{ee} represents the Coulomb interaction between two opposite-spin electrons on the center. $H_0 + H_{ee}$ represents the center by itself,

Parmenter, all m

the exact form of H_{ee} is

$$H_{ee} = \frac{1}{2} \sum_{m_1 m_2} \sum_{m_3 m_4} \sum_{s_1 s_2} \delta_{m_1+m_2, m_3+m_4} \langle m_3 m_4 | V | m_1 m_2 \rangle \times (c_{m_3 s_1} c_{m_4 s_2})^{\dagger} c_{m_1 s_1} c_{m_2 s_2} , \quad (11)$$

where

$$\langle m_3 m_4 | V | m_1 m_2 \rangle \equiv \int \int d^3 r_1 \, d^3 r_2 \, \psi^*_{m_3}(\vec{r}_1) \psi^*_{m_4}(\vec{r}_2) \times V(r_{12}) \psi_{m_1}(\vec{r}_1) \psi_{m_2}(\vec{r}_2) . \quad (12)$$

The rotational invariance properties of the H_{ee} are manifested by the fact that it commutes with the total spin angular momentum operator $\vec{S}$ and the total orbital angular momentum operator $\vec{L}$, where

$$\vec{S} = \sum_m \vec{S}_m$$

$$\vec{L} = \sum_s \vec{L}_s$$

$\vec{S}_m$ being the total spin angular momentum of all electrons in orbital m, and $\vec{L}_s$ being the total orbital angular momentum of all electrons of spin s.

Parmenter Hamiltonian 3

Following Anderson, we now assume that all nondiagonal values of Coulomb integral are the same and all nondiagonal values of exchange integral are the same, i. e.,

$$U_{mm'} = U, \quad J_{mm'} = J \qquad \text{if } m' \neq m \ . \tag{23}$$

Similarly, we assume all diagonal values are the same:

$$U_{mm} \equiv J_{mm} = U_0 \ . \tag{24}$$

Unlike Anderson, we do *not* assume U_0 is the same as U, but rather we choose U_0 and α such that

$$(1-\alpha)U_0 = U \ , \qquad \alpha U_0 = J \ , \tag{25}$$

so that

$$U_0 = (U+J) \ , \tag{26}$$

$$\alpha = J(U+J)^{-1} \ . \tag{27}$$

This choice ensures that $\bar{U}_{mm'} = U$ and $\bar{J}_{mm'} = J$ are both completely independent of m and m'. Thus,

$$H'_{ee} = (J - \tfrac{1}{2}U)N + \tfrac{1}{2}(U - \tfrac{1}{2}J)N^2 - J\vec{S}\cdot\vec{S} \ . \tag{28}$$

By inspection, H'_{ee} is invariant to rotations in both real and spin space. The rotational invariance in real space has been restored to H'_{ee} by the choice (26).

That portion of the total Hamiltonian describing the localized center by itself can be taken as

$$H_0 + H'_{ee} = (\epsilon_0 + J - \tfrac{1}{2}U)N + \tfrac{1}{2}(U - \tfrac{1}{2}J)N^2 - J\vec{S}\cdot\vec{S} \ . \tag{30}$$

references

[1] T. Dietl and H. Ohno, arXiv:1307.3429.

[2] A. Bonanni, M. Sawicki, T. Devillers, W. Stefanowicz, B. Faina, T. Li, T.E. Winkler, D. Sztenkiel, A. Navarro-Quezada, M. Rovezzi, R. Jakieła, A. Grois, M. Wegscheider, W. Jantsch, J. Suffczyński, F. D'Acapito, A. Meingast, G. Kothleitner, T. Dietl, Phys. Rev. B **84**, 035206 (2011)

[3] W. Stefanowicz, D. Sztenkiel, B. Faina, A. Grois, M. Rovezzi, T. Devillers, F. d'Acapito, A. Navarro-Quezada, T. Li, R. Jakieła, M. Sawicki, T. Dietl, A. Bonanni, Phys. Rev. B **81**, 235210 (2010)

[4] M. Sawicki, T. Devillers, S. Gałęski, C. Simserides, S. Dobkowska, B. Faina, A. Grois, A. Navarro-Quezada, K.N. Trohidou, J.A. Majewski, T. Dietl, A. Bonanni, Phys. Rev. B **85**, 205204 (2012)

[5] G. Kunert, S. Dobkowska, T. Li, H. Reuther, C. Kruse, S. Figge, R. Jakieła, A. Bonanni, J. Grenzer, W. Stefanowicz, J. von Borany, M. Sawicki, T. Dietl, D. Hommel, Appl. Phys. Lett. **101**, 022413 (2012)

[6] S. Stefanowicz, G. Kunert, C. Simserides, J.A. Majewski, W. Stefanowicz, C. Kruse, S. Figge, Tian Li, R. Jakieła, K.N. Trohidou, A. Bonanni, D. Hommel, M. Sawicki, T. Dietl, Phys. Rev. B **88**, 081201(R) (2013)

[7] A. Twardowski, H.J.M. Swagten, W.J.M. de Jonge, M. Demianiuk, Phys. Rev. B **36**, 7013 (1987); H.J.M. Swagten, A. Twardowski, P.J.T. Eggenkamp, W.J.M. de Jonge, ibid. **46**, 188 (1992)

[8] A. Lipińska, C. Simserides, K.N. Trohidou, M. Goryca, P. Kossacki, A. Majhofer, T. Dietl, Phys. Rev. B **79**, 235322 (2009)

[9] J. Blinowski, P. Kacman, J.A. Majewski, Phys. Rev. B **53**, 9524 (1996)

[10] R. Zallen, *The physics of amorphous solids*, Wiley-VCH Verlag GmbH & Co. KGaA, Weinheim, 2004

[11] G. Pollack, Rev. Mod. Phys. **36**, 748 (1964)

[12] C.D. Lorenz, R. May, R.M. Ziff, J. Stat. Phys. **98**, 961 (2000)

[13] M. Ferhat, A. Zaoui, M. Certier, B. Khelifa, Phys. Status Solidi B **195**, 415 (1996)

[14] J. Gosk, M. Zajac, A. Wolos, M. Kaminska, A. Twardowski,I. Grzegory, M. Bockowski, S. Porowski, Phys. Rev. B **71**, 094432 (2005)

[15] A. Stroppa and G. Kresse, Phys. Rev. B **79**, 201201(R) (2009)

[16] T. Graf, S.T.B. Goennenwein, M.S. Brandt, Phys. Status Solidi B **239**, 277 (2003)

[17] B. Han, B.W. Wessels, M.P. Ulmer, Appl. Phys. Lett. **86**, 042505 (2005)

[18] J.I. Hwang, Y. Ishida, M. Kobayashi, H. Hirata, K. Takubo, T. Mizokawa, A. Fujimori, J. Okamoto, K. Mamiya, Y. Saito, Y. Muramatsu, H. Ott, A. Tanaka, T. Kondo, H. Munekata, Phys. Rev. B **72**, 085216 (2005)

[19] M.E.J. Newman and G.T. Barkema, *Monte Carlo Methods in Statistical Physics*, Colorado Press, Oxford, 1999

[20] M. Matsumoto and T. Nishimura, ACM. Trans. Model. Comput. Simul. **8**, 3 (1998)

[21] K. Binder and D. W. Heermann, *Monte Carlo Simulation in Statistical Physics. An Introduction*, Springer Verlag, 1988

[22] E. Sarigiannidou, F. Wilhelm, E. Monroy, R. M. Galera, E. Bellet-Amalric, A. Rogalev, J. Goulon, J. Cibert, H. Mariette, Phys. Rev. B **74**, 041306 (2006)

[23] M. Sawicki, E. Guziewicz, M.I. Łukasiewicz, O. Proselkov,I. A. Kowalik, W. Lisowski, P. Dluzewski, A. Wittlin, M. Jaworski, A. Wolska, W. Paszkowicz, R. Jakiela, B. S. Witkowski, L. Wachnicki, M.T. Klepka, F.J. Luque, D. Arvanitis, J.W. Sobczak, M. Krawczyk, A. Jablonski, W. Stefanowicz, D. Sztenkiel, M. Godlewski, T. Dietl, Phys. Rev. B **88**, 085204 (2013)

[24] R. Rammal and J. Souletie, *Magnetism of Metals and Alloys*, North-Holland, Amsterdam, 1982

[25] T. Dietl, Phys. Rev. B **77**, 085208 (2008)

[26] K. Sato, L. Bergqvist, J. Kudrnovský, P.H. Dederichs, O. Eriksson, I. Turek, B. Sanyal, G. Bouzerar, H. Katayama-Yoshida, V.A. Dinh, T. Fukushima, H. Kizaki, R. Zeller, Rev. Mod. Phys. **82**, 1633 (2010)

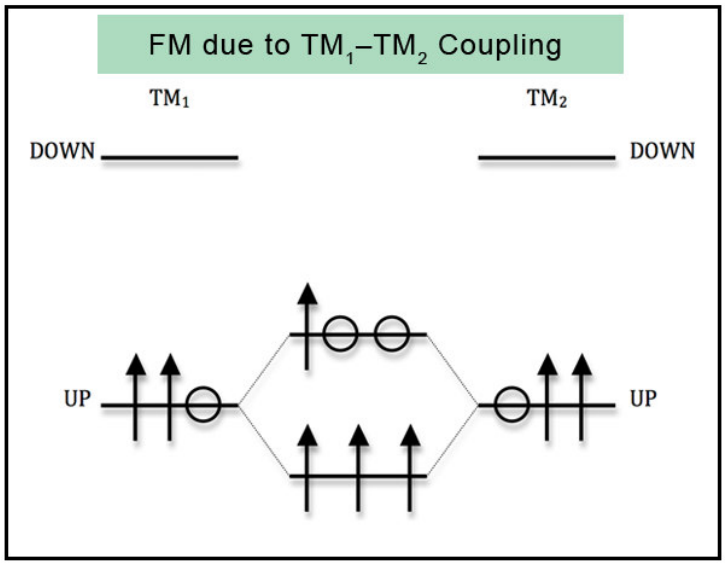

Energy level diagram describing the stabilization of the ferromagnetic spin arrangement as a result of the interaction between two hybrid orbitals located on two impurities, here labeled TM1 and TM2, in a **tetrahedral semiconductor**.
In the case of partial occupancy of the individual hybrid orbitals, the ferromagnetic configuration is stabilized by the preferential filling of the lower energy state.

Zunger Lany Raebiger Physics 3, 53 (2010)

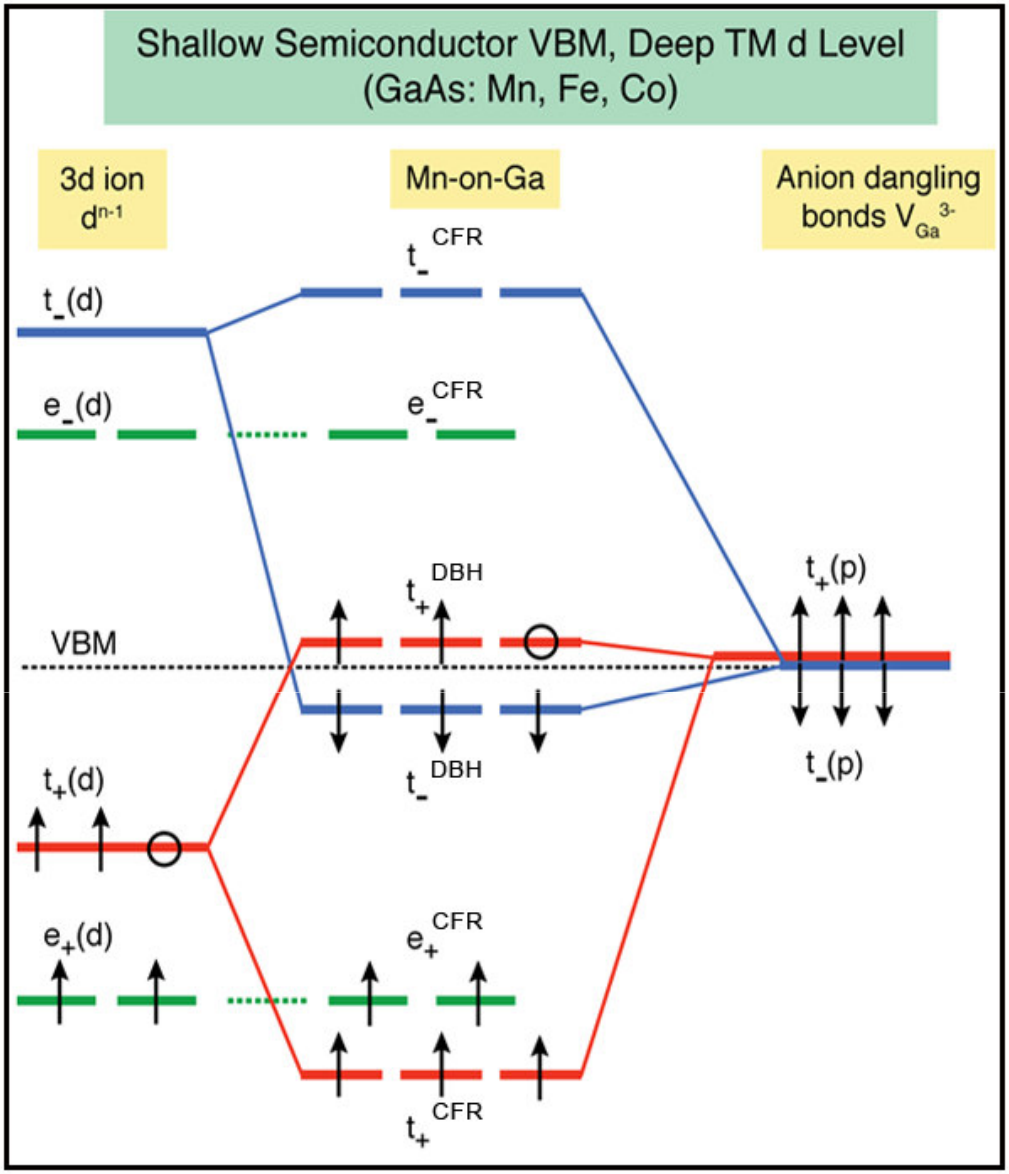

Energy level diagram describing how an individual hybrid orbital is formed from the coupling between the host cation vacancy orbitals t(p) and the 3d orbitals t(d)+e(d).

Transformational properties of atomic orbitals

- When bonds are formed, atomic orbitals combine according to their symmetry.
- Symmetry properties and degeneracy of orbitals and bonds can be learned from corresponding character tables by their inspection holding in mind the following transformational properties:

Atomic orbital	Transforms as
s	$x^2+y^2+z^2$
p_x	x
p_y	y
p_z	z
d_{z2}	z^2, $2z^2-x^2-y^2$
d_{x2-y2}	x^2-y^2
d_{xy}	xy
d_{xz}	xz
d_{yz}	yz

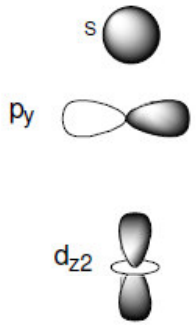

Mulliken labels

Polyatomic Molecular Orbital Theory

Atomic orbital	Mulliken labels				
	C_{2v}	D_{3h}	D_{4h}	T_d	O_h
s	a_1	a_1'	a_{1g}	a_1	a_{1g}
p_x	b_1	e'	e_u	t_2	t_{1u}
p_y	b_2	e'	e_u	t_2	t_{1u}
p_z	a_1	a_2''	a_{2u}	t_2	t_{1u}
d_{z2}	a_1	a_1'	a_{1g}	e	e_g
d_{x2-y2}	a_1	e'	b_{1g}	e	e_g
d_{xy}	a_2	e'	b_{2g}	t_2	t_{2g}
d_{xz}	b_1	e''	e_g	t_2	t_{2g}
d_{yz}	b_2	e''	e_g	t_2	t_{2g}

CFT

Crystal Field Theory (CFT)

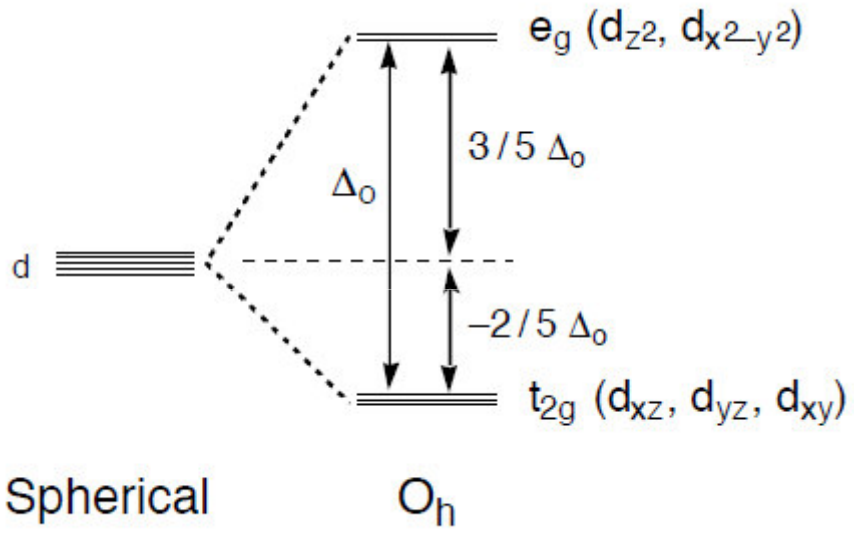

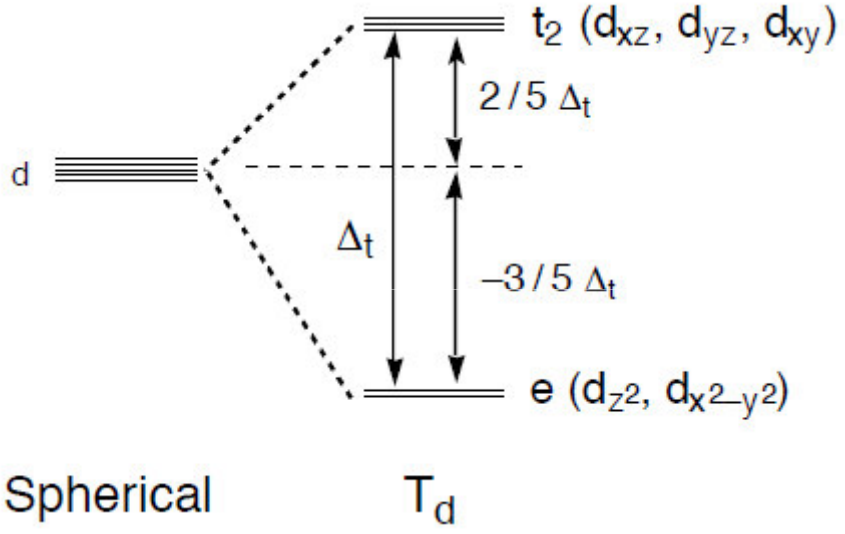

- http://chemistry.umeche.maine.edu/Modeling/mulliken.html
- http://www.adichemistry.com/inorganic/cochem/jahnteller/jahn-teller-distortion.html
- http://www.mpilkington.com/Lecture_7.pdf καλό
- http://chemistry.osu.edu/~ljoyce/Chem651/Chem651_part2.pdf **πολύ καλό**

PERIODIC TABLE

Atomic Properties of the Elements

NIST National Institute of Standards and Technology U.S. Department of Commerce

Physics Laboratory physics.nist.gov

Standard Reference Data www.nist.gov/srd

Frequently used fundamental physical constants

For the most accurate values of these and other constants, visit physics.nist.gov/constants

1 second = 9 192 631 770 periods of radiation corresponding to the transition between the two hyperfine levels of the ground state of ^{133}Cs

speed of light in vacuum	c	299 792 458 m s^{-1}	(exact)
Planck constant	h	6.6261 x 10^{-34} J s	($\hbar = h/2\pi$)
elementary charge	e	1.6022 x 10^{-19} C	
electron mass	m_e	9.1094 x 10^{-31} kg	
	$m_e c^2$	0.5110 MeV	
proton mass	m_p	1.6726 x 10^{-27} kg	
fine-structure constant	α	1/137.036	
Rydberg constant	R_∞	10 973 732 m^{-1}	
	$R_\infty c$	3.289 842 x 10^{15} Hz	
	$R_\infty hc$	13.6057 eV	
Boltzmann constant	k	1.3807 x 10^{-23} J K^{-1}	

Solids
Liquids
Gases
Artificially Prepared

Period	Group 1 IA	2 IIA	3 IIIB	4 IVB	5 VB	6 VIB	7 VIIB	8	9 VIII	10	11 IB	12 IIB	13 IIIA	14 IVA	15 VA	16 VIA	17 VIIA	18 VIIIA
1	1 $^2S_{1/2}$ **H** Hydrogen 1.00794 1s 13.5984																	2 $^1S_0$ **He** Helium 4.002602 $1s^2$ 24.5874
2	3 $^2S_{1/2}$ **Li** Lithium 6.941 $1s^2 2s$ 5.3917	4 $^1S_0$ **Be** Beryllium 9.012182 $1s^2 2s^2$ 9.3227											5 $^2P^o_{1/2}$ **B** Boron 10.811 $1s^2 2s^2 2p$ 8.2980	6 $^3P_0$ **C** Carbon 12.0107 $1s^2 2s^2 2p^2$ 11.2603	7 $^4S^o_{3/2}$ **N** Nitrogen 14.0067 $1s^2 2s^2 2p^3$ 14.5341	8 $^3P_2$ **O** Oxygen 15.9994 $1s^2 2s^2 2p^4$ 13.6181	9 $^2P^o_{3/2}$ **F** Fluorine 18.9984032 $1s^2 2s^2 2p^5$ 17.4228	10 $^1S_0$ **Ne** Neon 20.1797 $1s^2 2s^2 2p^6$ 21.5645
3	11 $^2S_{1/2}$ **Na** Sodium 22.98976928 [Ne]3s 5.1391	12 $^1S_0$ **Mg** Magnesium 24.3050 $[Ne]3s^2$ 7.6462											13 $^2P^o_{1/2}$ **Al** Aluminum 26.9815386 [Ne]3s^{2}3p 5.9858	14 $^3P_0$ **Si** Silicon 28.0855 $[Ne]3s^2 3p^2$ 8.1517	15 $^4S^o_{3/2}$ **P** Phosphorus 30.973762 $[Ne]3s^2 3p^3$ 10.4867	16 $^3P_2$ **S** Sulfur 32.065 $[Ne]3s^2 3p^4$ 10.3600	17 $^2P^o_{3/2}$ **Cl** Chlorine 35.453 $[Ne]3s^2 3p^5$ 12.9676	18 $^1S_0$ **Ar** Argon 39.948 $[Ne]3s^2 3p^6$ 15.7596
4	19 $^2S_{1/2}$ **K** Potassium 39.0983 [Ar]4s 4.3407	20 $^1S_0$ **Ca** Calcium 40.078 $[Ar]4s^2$ 6.1132	21 $^2D_{3/2}$ **Sc** Scandium 44.955912 $[Ar]3d4s^2$ 6.5616	22 $^3F_2$ **Ti** Titanium 47.867 $[Ar]3d^2 4s^2$ 6.8281	23 $^4F_{3/2}$ **V** Vanadium 50.9415 $[Ar]3d^3 4s^2$ 6.7462	24 $^7S_3$ **Cr** Chromium 51.9961 $[Ar]3d^5 4s$ 6.7665	25 $^6S_{5/2}$ **Mn** Manganese 54.938045 $[Ar]3d^5 4s^2$ 7.4340	26 $^5D_4$ **Fe** Iron 55.845 $[Ar]3d^6 4s^2$ 7.9024	27 $^4F_{9/2}$ **Co** Cobalt 58.933195 $[Ar]3d^7 4s^2$ 7.8810	28 $^3F_4$ **Ni** Nickel 58.6934 $[Ar]3d^8 4s^2$ 7.6399	29 $^2S_{1/2}$ **Cu** Copper 63.546 $[Ar]3d^{10} 4s$ 7.7264	30 $^1S_0$ **Zn** Zinc 65.38 $[Ar]3d^{10} 4s^2$ 9.3942	31 $^2P^o_{1/2}$ **Ga** Gallium 69.723 $[Ar]3d^{10} 4s^2 4p$ 5.9993	32 $^3P_0$ **Ge** Germanium 72.64 $[Ar]3d^{10} 4s^2 4p^2$ 7.8994	33 $^4S^o_{3/2}$ **As** Arsenic 74.92160 $[Ar]3d^{10} 4s^2 4p^3$ 9.7886	34 $^3P_2$ **Se** Selenium 78.96 $[Ar]3d^{10} 4s^2 4p^4$ 9.7524	35 $^2P^o_{3/2}$ **Br** Bromine 79.904 $[Ar]3d^{10} 4s^2 4p^5$ 11.8138	36 $^1S_0$ **Kr** Krypton 83.798 $[Ar]3d^{10} 4s^2 4p^6$ 13.9996
5	37 $^2S_{1/2}$ **Rb** Rubidium 85.4678 [Kr]5s 4.1771	38 $^1S_0$ **Sr** Strontium 87.62 $[Kr]5s^2$ 5.6949	39 $^2D_{3/2}$ **Y** Yttrium 88.90585 $[Kr]4d5s^2$ 6.2173	40 $^3F_2$ **Zr** Zirconium 91.224 $[Kr]4d^2 5s^2$ 6.6339	41 $^6D_{1/2}$ **Nb** Niobium 92.90638 $[Kr]4d^4 5s$ 6.7589	42 $^7S_3$ **Mo** Molybdenum 95.96 $[Kr]4d^5 5s$ 7.0924	43 $^6S_{5/2}$ **Tc** Technetium (98) $[Kr]4d^5 5s^2$ 7.28	44 $^5F_5$ **Ru** Ruthenium 101.07 $[Kr]4d^7 5s$ 7.3605	45 $^4F_{9/2}$ **Rh** Rhodium 102.90550 $[Kr]4d^8 5s$ 7.4589	46 $^1S_0$ **Pd** Palladium 106.42 $[Kr]4d^{10}$ 8.3369	47 $^2S_{1/2}$ **Ag** Silver 107.8682 $[Kr]4d^{10} 5s$ 7.5762	48 $^1S_0$ **Cd** Cadmium 112.411 $[Kr]4d^{10} 5s^2$ 8.9938	49 $^2P^o_{1/2}$ **In** Indium 114.818 $[Kr]4d^{10} 5s^2 5p$ 5.7864	50 $^3P_0$ **Sn** Tin 118.710 $[Kr]4d^{10} 5s^2 5p^2$ 7.3439	51 $^4S^o_{3/2}$ **Sb** Antimony 121.760 $[Kr]4d^{10} 5s^2 5p^3$ 8.6084	52 $^3P_2$ **Te** Tellurium 127.60 $[Kr]4d^{10} 5s^2 5p^4$ 9.0096	53 $^2P^o_{3/2}$ **I** Iodine 126.90447 $[Kr]4d^{10} 5s^2 5p^5$ 10.4513	54 $^1S_0$ **Xe** Xenon 131.293 $[Kr]4d^{10} 5s^2 5p^6$ 12.1298
6	55 $^2S_{1/2}$ **Cs** Cesium 132.9054519 [Xe]6s 3.8939	56 $^1S_0$ **Ba** Barium 137.327 $[Xe]6s^2$ 5.2117	57–71 Lanthanides	72 $^3F_2$ **Hf** Hafnium 178.49 $[Xe]4f^{14} 5d^2 6s^2$ 6.8251	73 $^4F_{3/2}$ **Ta** Tantalum 180.94788 $[Xe]4f^{14} 5d^3 6s^2$ 7.5496	74 $^5D_0$ **W** Tungsten 183.84 $[Xe]4f^{14} 5d^4 6s^2$ 7.8640	75 $^6S_{5/2}$ **Re** Rhenium 186.207 $[Xe]4f^{14} 5d^5 6s^2$ 7.8335	76 $^5D_4$ **Os** Osmium 190.23 $[Xe]4f^{14} 5d^6 6s^2$ 8.4382	77 $^4F_{9/2}$ **Ir** Iridium 192.217 $[Xe]4f^{14} 5d^7 6s^2$ 8.9670	78 $^3D_3$ **Pt** Platinum 195.084 $[Xe]4f^{14} 5d^9 6s$ 8.9588	79 $^2S_{1/2}$ **Au** Gold 196.966569 $[Xe]4f^{14} 5d^{10} 6s$ 9.2255	80 $^1S_0$ **Hg** Mercury 200.59 $[Xe]4f^{14} 5d^{10} 6s^2$ 10.4375	81 $^2P^o_{1/2}$ **Tl** Thallium 204.3833 [Hg]6p 6.1082	82 $^3P_0$ **Pb** Lead 207.2 $[Hg]6p^2$ 7.4167	83 $^4S^o_{3/2}$ **Bi** Bismuth 208.98040 $[Hg]6p^3$ 7.2855	84 $^3P_2$ **Po** Polonium (209) $[Hg]6p^4$ 8.414	85 $^2P^o_{3/2}$ **At** Astatine (210) $[Hg]6p^5$	86 $^1S_0$ **Rn** Radon (222) $[Hg]6p^6$ 10.7485
7	87 $^2S_{1/2}$ **Fr** Francium (223) [Rn]7s 4.0727	88 $^1S_0$ **Ra** Radium (226) $[Rn]7s^2$ 5.2784	89–103 Actinides	104 $^3F_2$? **Rf** Rutherfordium (265) $[Rn]5f^{14} 6d^2 7s^2$ 6.0?	105 **Db** Dubnium (268)	106 **Sg** Seaborgium (271)	107 **Bh** Bohrium (272)	108 **Hs** Hassium (277)	109 **Mt** Meitnerium (276)	110 **Ds** Darmstadtium (281)	111 **Rg** Roentgenium (280)	112 **Cn** Copernicium (285)	113 **Uut** Ununtrium (284)	114 **Uuq** Ununquadium (289)	115 **Uup** Ununpentium (288)	116 **Uuh** Ununhexium (293)	117 **Uus** Ununseptium (294)	118 **Uuo** Ununoctium (294)

Lanthanides

57 $^2D_{3/2}$ **La** Lanthanum 138.90547 [Xe]5d6s^2 5.5769	58 $^1G^o_4$ **Ce** Cerium 140.116 $[Xe]4f5d6s^2$ 5.5387	59 $^4I^o_{9/2}$ **Pr** Praseodymium 140.90765 $[Xe]4f^3 6s^2$ 5.473	60 $^5I_4$ **Nd** Neodymium 144.242 $[Xe]4f^4 6s^2$ 5.5250	61 $^6H^o_{5/2}$ **Pm** Promethium (145) $[Xe]4f^5 6s^2$ 5.582	62 $^7F_0$ **Sm** Samarium 150.36 $[Xe]4f^6 6s^2$ 5.6437	63 $^8S^o_{7/2}$ **Eu** Europium 151.964 $[Xe]4f^7 6s^2$ 5.6704	64 $^9D^o_2$ **Gd** Gadolinium 157.25 $[Xe]4f^7 5d6s^2$ 6.1498	65 $^6H^o_{15/2}$ **Tb** Terbium 158.92535 $[Xe]4f^9 6s^2$ 5.8638	66 $^5I_8$ **Dy** Dysprosium 162.500 $[Xe]4f^{10} 6s^2$ 5.9389	67 $^4I^o_{15/2}$ **Ho** Holmium 164.93032 $[Xe]4f^{11} 6s^2$ 6.0215	68 $^3H_6$ **Er** Erbium 167.259 $[Xe]4f^{12} 6s^2$ 6.1077	69 $^2F^o_{7/2}$ **Tm** Thulium 168.93421 $[Xe]4f^{13} 6s^2$ 6.1843	70 $^1S_0$ **Yb** Ytterbium 173.054 $[Xe]4f^{14} 6s^2$ 6.2542	71 $^2D_{3/2}$ **Lu** Lutetium 174.9668 $[Xe]4f^{14} 5d6s^2$ 5.4259

Actinides

89 $^2D_{3/2}$ **Ac** Actinium (227) [Rn]6d7s^2 5.3807	90 $^3F_2$ **Th** Thorium 232.03806 $[Rn]6d^2 7s^2$ 6.3067	91 $^4K_{11/2}$ **Pa** Protactinium 231.03588 $[Rn]5f^2 6d7s^2$ 5.89	92 $^5L^o_6$ **U** Uranium 238.02891 $[Rn]5f^3 6d7s^2$ 6.1939	93 $^6L_{11/2}$ **Np** Neptunium (237) $[Rn]5f^4 6d7s^2$ 6.2657	94 $^7F_0$ **Pu** Plutonium (244) $[Rn]5f^6 7s^2$ 6.0260	95 $^8S^o_{7/2}$ **Am** Americium (243) $[Rn]5f^7 7s^2$ 5.9738	96 $^9D^o_2$ **Cm** Curium (247) $[Rn]5f^7 6d7s^2$ 5.9914	97 $^6H^o_{15/2}$ **Bk** Berkelium (247) $[Rn]5f^9 7s^2$ 6.1979	98 $^5I_8$ **Cf** Californium (251) $[Rn]5f^{10} 7s^2$ 6.2817	99 $^4I^o_{15/2}$ **Es** Einsteinium (252) $[Rn]5f^{11} 7s^2$ 6.3676	100 $^3H_6$ **Fm** Fermium (257) $[Rn]5f^{12} 7s^2$ 6.50	101 $^2F^o_{7/2}$ **Md** Mendelevium (258) $[Rn]5f^{13} 7s^2$ 6.58	102 $^1S_0$ **No** Nobelium (259) $[Rn]5f^{14} 7s^2$ 6.65	103 $^2P^o_{1/2}$? **Lr** Lawrencium (262) $[Rn]5f^{14} 7s^2 7p$? 4.9 ?

Atomic Number — Ground-state Level
Symbol
Name
Atomic Weight†
Ground-state Configuration
Ionization Energy (eV)

58 $^1G^o_4$ **Ce** Cerium 140.116 $[Xe]4f5d6s^2$ 5.5387

†Based upon ^{12}C. ( ) indicates the mass number of the longest-lived isotope.

For a description of the data, visit physics.nist.gov/data

NIST SP 966 (September 2010)

Jahn Teller distortions

- http://www.adichemistry.com/inorganic/cochem/jahnteller/jahn-teller-distortion.html
- http://chemwiki.ucdavis.edu/Inorganic_Chemistry/Coordination_Chemistry/Coordination_Numbers/Jahn-Teller_Distortions

Usually octahedral
d^4 high spin

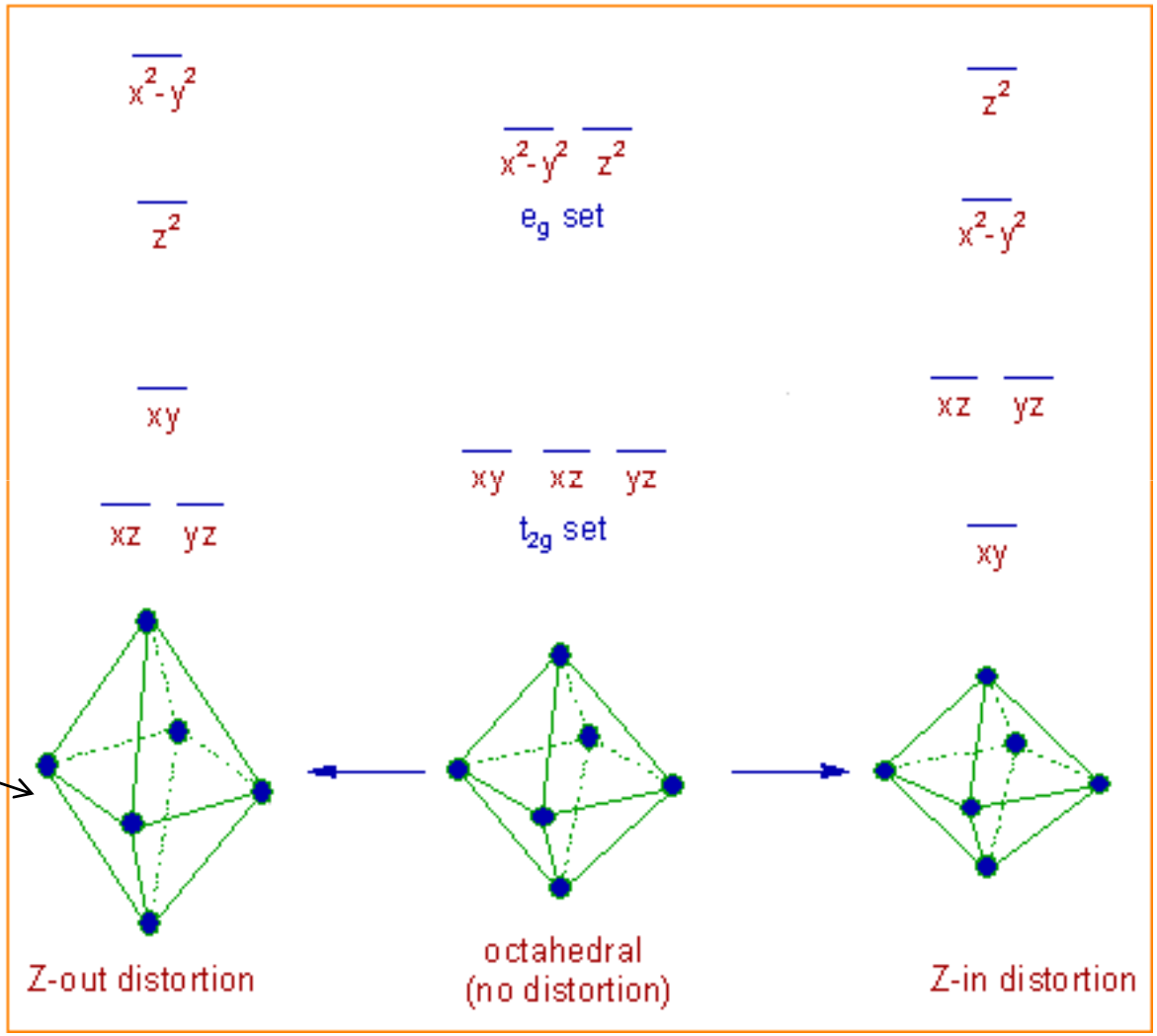

types of exchange . . .

potential exchange

kinetic exchange

superexchange

sp–d Zener or RKKY mechanism

double-exchange

Stoner mechanism

. . .

Dietl and Ohno arXiv 1307.3429v2

Bonanni and Dietl Chem. Soc. Rev. 39 (2010) 528

(a) superexchange vs. (b) double exchange

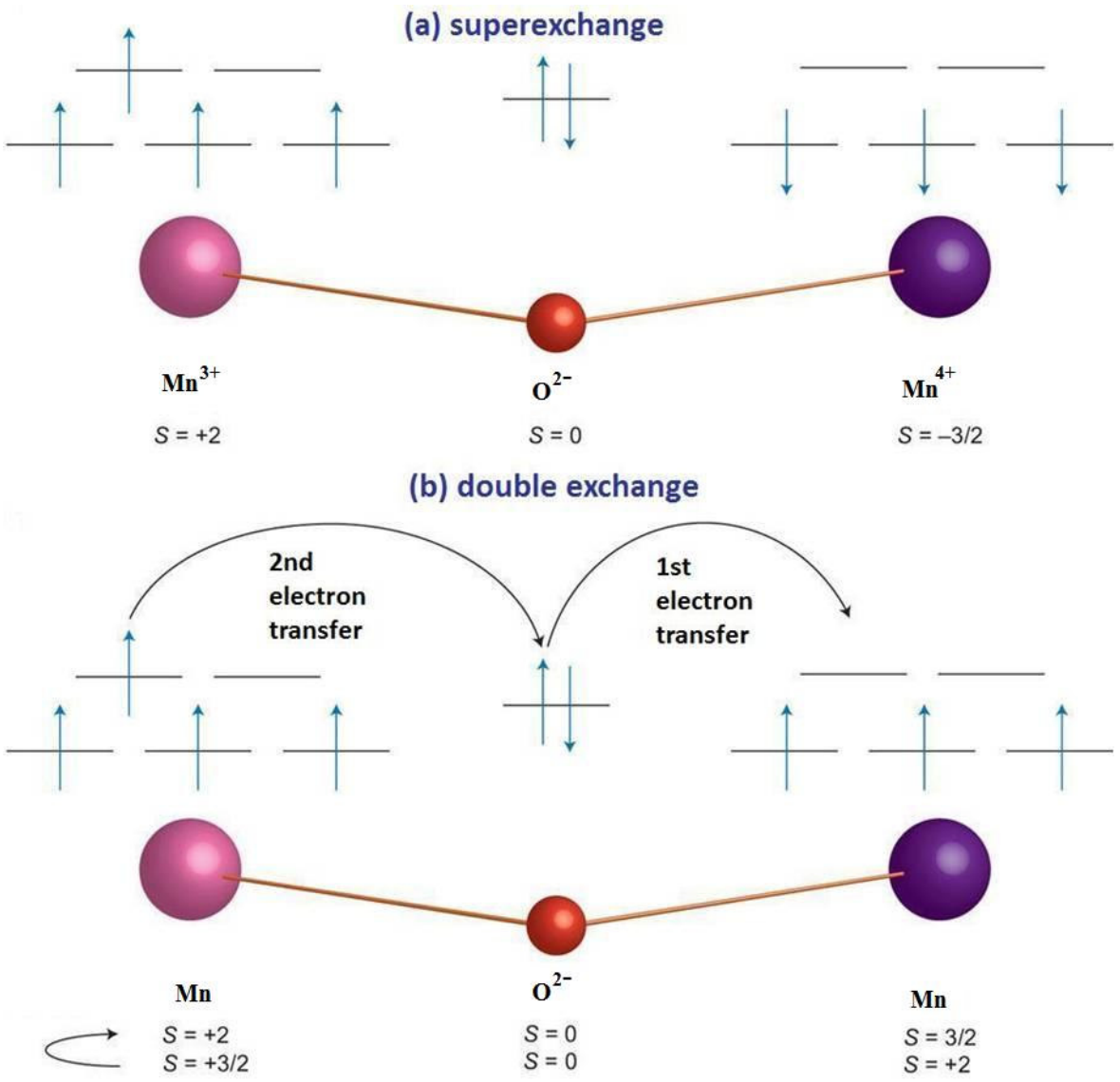

Figure from Annie K. Powell Nature Chemistry **2**, 351 (2010)
"Molecular magnetism: A bridge to higher ground"

[a] Superexchange: localized system

electrons remain in their orbitals

spin info transferred according to symmetry

-here *antiferromagnetic* superexchange-

mediated by a pair of electrons on O^{2-}

[b] Double-exchange: simultaneous transfer of two electrons

1st e.g. "spin up" from O^{2-} to Mn^{4+}

2nd "spin up" from Mn^{3+} to O^{2-}

ferromagnetic info transferred back and forth by itinerant electrons

(c) carrier-mediated coupling (sp-d Zener or RKKY mechanism)

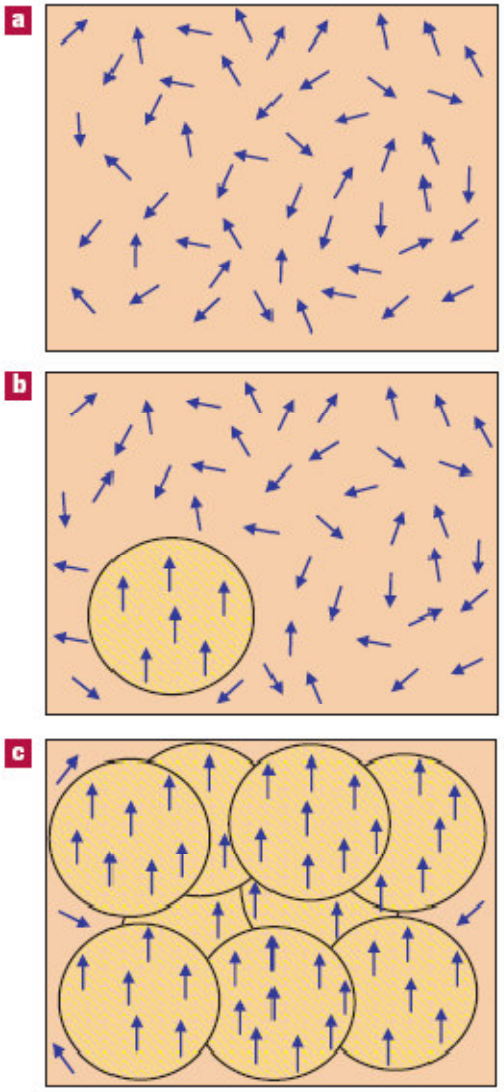

Holes induce Ferromagnetism!

(Ga,Mn)As

Figure from Jungwirth et al., Rev. Mod. Phys. 78 (2006) 809

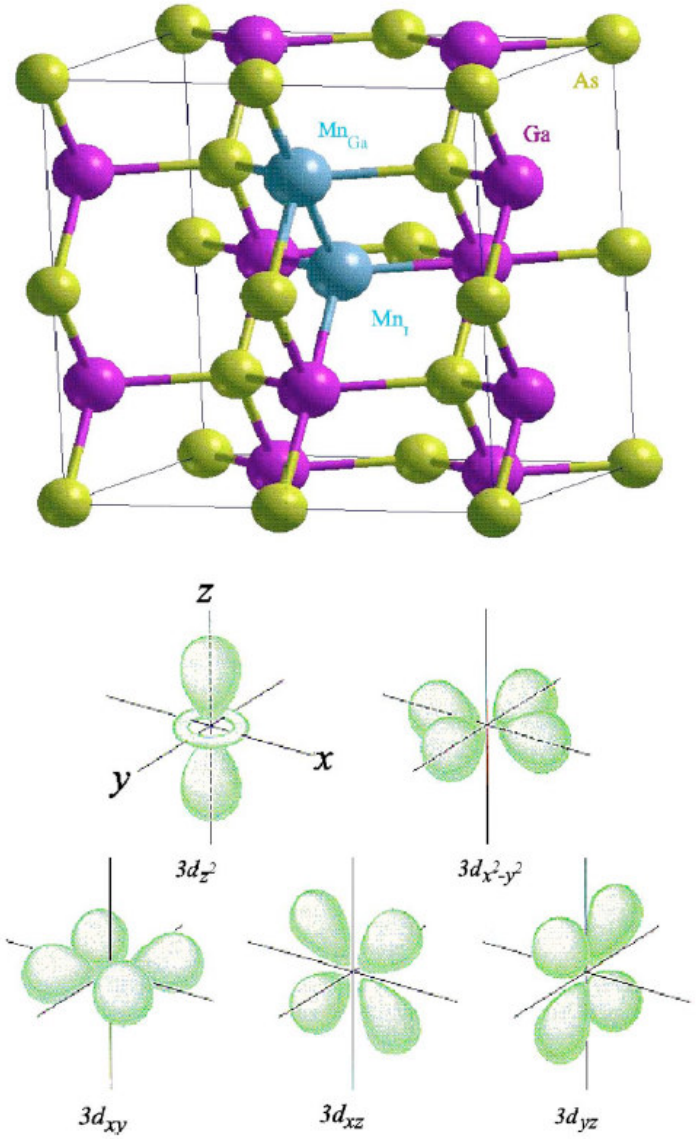

FIG. 3. (Color online) Top panel: Substitutional Mn_{Ga} and interstitial Mn_I in GaAs. Bottom panel: Two e_g $3d$ orbitals and three t_{2g} $3d$ orbitals of Mn.

$$r_n = \begin{cases} D\sqrt{n}, & n \le 13 \\ D\sqrt{n+1}, & 14 \le n \le 16 \end{cases}$$

Table 1: The two sets of J_{ij} used. The columns contain the order of neighbors, the number of atoms z_n centered at a distance r_n from a given atom, the distance between neighbors r_n measured in D, the 1st set of J_{ij} and the 2nd set of J_ij measured in Kelvin and a representative vector or the class $R(C_n)$ measured in $[a_0/2]$ (cf. subsection2.1).

order	z_n	r_n	J_{ij} (K)	J_{ij} (K)	a vector
1st	12	1	8.8340	27.3684	(1,1,0)
2nd	6	$\sqrt{2}$	0.5569	1.8190	(2,0,0)
3rd	24	$\sqrt{3}$	1.0916	2.9216	(2,1,1)
4th	12	2	1.0088	2.6552	(2,2,0)
5th	24	$\sqrt{5}$	0.0467	0.1258	(3,1,0)
6th	8	$\sqrt{6}$	0.1402	0.3661	(2,2,2)
7th	48	$\sqrt{7}$	0.0971	0.2544	(3,1,2)
8th	6	$\sqrt{8}$	0.0017	0.0046	(4,0,0)
9th	12	3	0.0770	0.2028	(3,3,0)
	24		0.0054	0.0144	(4,1,1)
10th	24	$\sqrt{10}$	0.0082	0.0219	(4,2,0)
11th	24	$\sqrt{11}$		0.0514	(3,3,2)
12th	24	$\sqrt{12}$		0.0300	(4,2,2)
13th	24	$\sqrt{13}$		0.0015	(5,1,0)
	48			0.0289	(4,1,3)
14th	48	$\sqrt{15}$		0.0029	(5,1,2)
15th	12	4		0.0197	(4,4,0)
16th	24	$\sqrt{17}$		0.0037	(5,3,0)
	24			0.0088	(4,3,3)
sum	428				

The Heisenberg Hamiltonian used reads

$$\mathcal{H}_{dd} = -k_B \sum_{i<j} J_{ij} \mathbf{S}_i \cdot \mathbf{S}_j. \tag{7}$$

k_B is the Boltzmann constant. We treat the Mn^{+3} spins $\mathbf{S}_i$, $\mathbf{S}_j$ as classical vectors with norm $S = 2$. At each Monte Carlo (MC) sweep, the mean spin projections ($l = x, y, z,$) and the mean spin norm

$$\overline{S_l} = \frac{\sum_{i=1}^{N} S_{il}}{N}, \quad \overline{S} = \frac{\sum_{i=1}^{N} S_i}{N}. \tag{8}$$

are calculated. $N = N_{\mathrm{Mn}}$ is the number of Mn ions. Hence, we denote mean values (i.e. per Mn ion) by $\overline{\cdots}$. We denote statistical averages [44] by $\langle \cdots \rangle$, i.e.

$$\langle S_l \rangle = \frac{\sum_{n=1}^{n_t} \overline{S_l}}{n_t}, \quad \langle S \rangle = \frac{\sum_{n=1}^{n_t} \overline{S}}{n_t}. \tag{9}$$

n (n_t) denotes successive (the total number of) MC sweeps used for the statistical average. Similarly, for any integer p one could define

$$\langle S^p \rangle = \frac{\sum_{n=1}^{n_t} \overline{S}^p}{n_t}. \tag{10}$$

The spin susceptibility components per spin (χ_{S_l}) and the spin susceptibility per spin (χ_S) read [44]

$$\chi_{S_l} = \frac{N}{T}[\langle S_l^2 \rangle - \langle S_l \rangle^2], \quad \chi_S = \frac{N}{T}[\langle S^2 \rangle - \langle S \rangle^2]. \tag{11}$$

Method of J_{ij} calculation

Average over 9 possible pairs of Mn *d* orbitals (d_{yz}, d_{zx}, d_{xy})
for a class (shell) of neighbors of the given lattice site assumed to be the site (0,0,0)

$$\bar{J}(C_n) = \frac{1}{9}\sum_{\gamma,\delta=1}^{3} J_{xx}^{\gamma\delta}(\vec{R}(C_n))$$

$J_{xx}^{\gamma\delta}(\vec{R}(C_n))$ is the exchange integral for the Mn-Mn distance defined by $\vec{R}(C_n)$
C_n is the *n*th shell of the lattice site (or atom) at (0,0,0).
It consists of lattice points that have the same distance to the point (0,0,0) and can be transformed to each other by a symmetry operation of the point group O_h.
The shell (class) defined that way cannot consist of more than 48 *R vectors.*

$$J_{xx}^{\gamma\delta}(\vec{R}(C_n)) = J_{yy}^{\gamma\delta}(\vec{R}(C_n)) = J_{zz}^{\gamma\delta}(\vec{R}(C_n)).$$

$$J_{\alpha\beta}^{\gamma\delta}(\vec{R}(C_n)) = 0, \text{ for } \alpha \neq \beta.$$

$$C_n=\{\vec{R}_j,\ j=1,\ldots,N_n\ |\vec{R}_j|=d_n, \forall_{i,j}\ \vec{R}_j=\hat{P}\vec{R}_i,\ \hat{P}\in O_h\}.$$

A vector belonging to the class C_n *is denoted by*
Further, $\gamma(\delta) = 1 \equiv yz$, $\gamma(\delta) = 2 \equiv zx$, $\gamma(\delta) = 3 \equiv xy$.
The Tight-Binding calculations are performed for zincblende GaN, i.e. the cationic sublattice is fcc. The integrals over the Brillouin zone have been performed using 2048 *k*-points. This guarantees that J_{ij} are computed with an accuracy of 0.0002 K.

End of back up